REVIEW OF MODELS TO PREDICT INTERNAL PITTING CORROSION OF OIL AND GAS PIPELINES

Sankara Papavinasam¹, R. Winston Revie¹, Waldemar I. Friesen²,
Alex Doiron and Tharani Panneerselvam¹

Natural Resources Canada

CANMET Materials Technology Laboratory
568 Booth Street, Ottawa, Ontario K1A 0G1
Canada

CANMET Energy Technology Centre
1 Oil Patch Drive, Devon, Alberta T9G-1A8
Canada

ABSTRACT

Internal pitting corrosion is a significant factor in the degradation of pipelines used for oil and gas production. The penetration of the pipe wall by pits is a process that consists of three stages: formation of a passive layer on the steel surface, initiation of pits at localized regions on the steel surface where film breakdown occurs, and pit propagation and eventual penetration of the pipe wall. This paper reviews the various models (based on corrosion science, electrochemical science, and corrosion engineering approach) that can be used to predict internal pitting corrosion of oil and gas pipelines.

Models that have been developed based on laboratory experiments are analysed to assess the effects of experimental duration, apparatus, and conditions on the results. Electrochemical reactions are involved in all three stages. Applicability of electrochemical models to predict internal pitting corrosion of pipelines is analysed. Analysis of time-series data from oil and gas fields indicated no significant differences in superficial oil, water, and gas velocities and watercut between pipelines that had failed and those that had not. Additionally, there is no correlation of other operating parameters, such as pipe inclination, operating pressure (both maximum and average) and hydrogen sulfide (H₂S), with pit growth rates.

None of the three models cover all elements of pitting corrosion, but each

one of them has a few advantages on certain aspects of pitting corrosion. A general approach to integrate the three types is outlined.

INTRODUCTION

Internal corrosion, particularly pitting corrosion, of carbon and low-alloy steels caused by carbon dioxide (CO₂) and H₂S is a major threat to the integrity of pipelines. Thus, there is a need to determine the risk due to internal pitting corrosion when designing production equipment and transportation facilities /l. In this paper, the models that can be used to assess and manage the risk of internal pitting corrosion of production equipment and production facilities are reviewed. According to the U.S. Office of Pipeline Safety, internal corrosion was responsible for 15% of all transmission pipeline incidents between 1994 and 2004 in the U.S.A /2/. According to the Alberta Energy and Utilities Board (AUEB) /3/, there were 808 failures between April 2001 and March 2002, of which 425 (52.7%) resulted from internal corrosion. The total number of failures in Alberta, Canada due to internal pitting corrosion in both gathering and transmission pipelines (gas and liquid) for the past 20 years are more than 5,000, averaging almost 1 failure per day /3/.

An industry-standard approach for assessing the risk of internal pitting corrosion does not exist at the present time, although there are references in publications of the National Gasoline Association of America, American Petroleum Institute, and Canadian Standards Association /4/. Recently, the Canadian Association of Petroleum Producers (CAPP) published standard practices to control internal pitting corrosion of sweet and sour pipelines /5.6/.

To effectively control internal pitting corrosion, field operators require a predictive tool that can be applied at all stages of project development and operation. Such a tool should answer the following six questions:

- 1. Does internal corrosion pose a significant risk?
- 2. If so, when during operation is a failure likely to occur?
- 3. Where in the pipeline is the failure likely to occur?
- 4. What is the failure mechanism likely to be?
- 5. Which operating parameters should be monitored to accurately predict the failure?

6. How can the predictions be validated and utilized in a user-friendly manner?

The approaches that have been developed to answer these questions can be classified broadly into methods based on corrosion science /7/, electrochemical science /8/, and corrosion engineering /9/. In this paper, the currently existing models are reviewed.

CORROSION SCIENCE MODELS

The corrosion science approach to developing models that predict the internal pitting corrosion of oil and gas pipelines involves the following steps:

- The factors influencing corrosion are assumed.
- Laboratory experiments are carried out to determine the extent of the influence of these parameters on corrosion rates.
- A theoretical explanation (based on corrosion kinetics and/or thermodynamics) is developed.
- The influences of various parameters are integrated.

Twelve corrosion science models are discussed below.

De Waard-Milliams Models

The model developed by de Waard and Milliams is the most-frequently referenced model used to evaluate internal corrosion /10/. The first version of this model was published in 1975, and it has since been revised three times.

Corrosion rates were determined in the laboratory using polished cylindrical X-52 carbon steel specimens in a 0.1% NaCl solution, saturated with CO_2 and oxygen-free N_2 . The corrosion rate was monitored using the linear polarization technique. Experiments were also performed in an autoclave for seven days, and mass losses were determined /10/.

Some of the electrodes, particularly at temperatures above 60°C, became covered with a black layer, while the corrosion rate decreased. In a stagnant environment, this effect was observed even at 40°C. To account for the changes in CO₂ solubility and the dissociation constant, the pH was measured

175

as a function of temperature for $pCO_2 = 1$ bar (corrected for water vapour pressure).

At a constant pH level, the effect of temperature on corrosion rate is characterized by an activation energy of 10.7 kcal/mole. Based on these simple experiments, it was concluded that the corrosion rate of carbon steel as a function of CO₂ partial pressure and temperature could be predicted, provided that passivation does not occur. Both the de Waard-Milliams equation and the nomogram that was subsequently developed have gained wide acceptance. Additionally, correctional factors were introduced to account for the effects of total pressure, scaling, and hydrocarbons.

In the earlier versions of the model, there was no significant consideration of the effects of liquid flow velocity on the CO₂ corrosion rate. The corrosion reaction was assumed to be activation-controlled, although the observed corrosion rates were, in some cases, about twice the rate predicted /11/. Therefore, a semi-empirical equation was developed to describe and predict the effect of the flow rate.

In 1995, the effect of carbides on the CO₂ corrosion rate was addressed, with a stipulation that the modification proposed (which would account for differences between various low-alloy steels) should be regarded as tentative and that it would only apply under conditions where protective films do not form /12/.

This model can be used to predict conditions at which an iron carbonate (FeCO₃) surface layer will be formed.

Srinivasan Model

The basis of the Srinivasan model /13/ is the de Waard-Milliams relationship between CO₂ and corrosion rate, but additional correction factors are introduced. The first step in this approach is a computation of the system pH. The dissolved CO₂ (or H₂S) that contributes to pH is determined as a function of acid gas partial pressures, bicarbonates and temperature.

In addition to pH reduction, the Srinivasan Model takes into account the following three-fold role of H₂S /13/:

- At very low levels of H₂S (<0.01 psia), CO₂ is the dominant corrosive species. At temperatures above 60°C, corrosion and passivity depend on FeCO₃ formation.
- At temperatures below 120°C, the presence of even a small amount of

 H_2S (ratio of pCO₂/pH₂S > 200) can lead to the formation of an iron sulphide layer, mackinawite. This mackinawite layer, which is produced on the metal surface as a function of the reaction between Fe and S, is influenced by both pH and temperature. This surface reaction can lead to the formation of a thin surface layer that can mitigate corrosion.

 For pCO₂/pH₂S < 200, a metastable sulphide layer forms in preference to the FeCO₃ layer. In the temperature range between 60 and 240°C, this layer is protective, provided that the layer contains no holidays or cracks.

At temperatures below 60°C or above 240°C, the presence of H₂S accelerates corrosion in steels because H₂S prevents the formation of a stable FeCO₃ layer; FeS then becomes unstable and porous and does not provide protection. In addition, the influence of various other parameters are integrated including an increase in the maximum operating temperature, dissolved chlorides, increase in the gas-to-oil ratio, increase in the water-to-gas ratio/water cut, oil type and its persistence, elemental sulphur/aeration, increase in fluid velocity, change in the type of flow, and inhibitor type and efficiency.

This model is useful in determining the regions of stability of both FeCO₃ and FeS layers.

Crolet Model

The Crolet model /14,15/ predicts the probability of corrosion in oil wells. It is based on a detailed analysis of field data on CO₂ corrosion from two oil field operations.

Crolet stated that three complementary conditions are necessary for internal pitting corrosion to occur /14/:

- 1. Water must be present and in contact with the metal;
- 2. The water must have a sufficient "potential corrosivity" (PC); and
- Conditions must be favourable for corrosion to develop locally, that is, active anodic sites must remain stable near protected or slowly corroding areas /9,10/.

In water-cuts between 25 and 40%, the risk of corrosion remains low at moderate flow rates and low pressure. At high pressure, corrosion occurs at water-cuts of 0.5 to 5%.

Potential corrosivity is defined as the maximum uniform corrosion rate that could be produced by the medium in the absence of any protective effect. The corrosion rate will remain low if the potential corrosivity is low. On the other hand, high potential corrosivity does not necessarily imply a higher rate of corrosion. Potential corrosivity represents the maximum possible corrosion rate of carbon steel in a CO₂-containing medium. It is, therefore, a parameter that can be readily measured in the laboratory.

In the Crolet model the parameters that influence potential corrosivity are: pH level, H₂CO₃, CO₂, acetic acid, temperature, and flow rate.

The potential corrosivity values of the Crolet model and the corrosion rates given by the de Waard and Milliams nomograms are very similar and show good overall agreement.

The nature and physical chemistry of CO₂-containing production waters influence localized corrosion. Whereas laboratory experiments can be carried out to measure the potential corrosivity of CO₂-containing media, localized CO₂ corrosion has proven to be extremely difficult to reproduce. The Crolet model identifies three categories of wells /14,15/:

- 1. Corrosive (C): Wells with a lifetime of less than two to three years.
- 2. Possibly corrosive (P): Wells with potential corrosion problems.
- Non-corrosive (N): Wells in which no corrosion problems have been encountered over a period of at least eight years, in spite of significant water cut.

This model defines the conditions for the formation of FeCO₃ and the influence of acetic acid on its stability.

Nesic Models

Nesic used a theoretical approach by modelling individual electrochemical reactions occurring in a water-CO₂ system /16/. The processes modelled in this system are the electrochemical reactions at the metal surface and the transport processes of all the species in the system, including H⁺, CO₂, H₂CO₃, and Fe²⁺.

Version 1 of the Nesic model focuses on the electrochemical reactions occurring in an acidic solution with dissolved CO₂. Glass-cell experiments were used to study the corrosion mechanisms and to determine the constants used in the model. The experimental results were then used to propose a

mechanistic CO₂ corrosion model.

The Nesic model requires the following inputs: temperature, pH, CO₂ partial pressure, oxygen concentration, steel, and flow geometry.

The predictions of this model are similar to the 1995 version of the de Waard and Milliams model. Most of the constants in the Nesic model can be determined experimentally, and they are physically relevant. Since the model is theoretical, it can be expanded to include other corrosion-influencing factors, e.g., transport processes. This could lead to more accurate predictions of protective film formation or the inclusion of an inhibitor effect in a physically meaningful way /16,17/.

When the concentrations of Fe²⁺ and CO₃²⁻ ions exceed the solubility limit, they combine to form solid iron carbonate films. Nucleation of crystalline films is a very difficult process to model mathematically. Additionally, in many corrosion situations, the rate of precipitation is considered to be controlled by the crystal growth rate, rather than the nucleation rate.

Version 2 of the Nesic model /18/ can be used to predict the equivalent of a scaling tendency (that is, the ratio between the precipitation rate and the corrosion rate) before any film is formed.

Using this model, two main cases of scaling can be identified:

- 1. When the precipitation rate is much lower than the corrosion rate (expressed in the same units), the result is a porous and unprotective film.
- 2. When the precipitation rate is much higher than the corrosion rate, a dense protective iron carbonate film forms.

The film thickness and porosity have been correlated empirically with results from corrosion loop experiments /16,18/. It is recognized that protective iron-carbonate corrosion-product films are crucial in predicting the actual corrosion rate at higher temperatures and pH, and that mechanistic modelling of the morphology of these corrosion films is a difficult task. The weaknesses of the model are primarily related to the lack of reliable experimental data at higher temperatures and CO₂ partial pressures. Additionally, the effects related to the presence of conducting surface films (e.g., iron carbide or iron sulphide) need to be introduced.

Mishra Model

Corrosion of steel in CO₂ solutions is considered to be a chemical-reaction-controlled process. In the Mishra model /19/, a corrosion-rate equation was derived on the basis of fundamental reaction rate theory and was then compared with empirically determined relationships reported in the literature /10/. The prediction of this model is similar to the empirically developed models; the model, however, accounts for the effects of steel microstructure and the flow velocity of the solution on the corrosion rate. The application limit for this model occurs when the corrosion process begins to be diffusion-controlled, usually after the formation of a stable corrosion product scale on the steel surface /19/.

Anderko Model

This model /20/ has been developed to calculate the corrosion rates of carbon steels in the presence of CO₂, H₂S, and brine. It combines a thermodynamic model (that provides realistic speciation of aqueous systems) with an electrochemical model (based on partial cathodic and anodic processes on the metal surface). The partial processes taken into account by this model include the oxidation of iron and reduction of hydrogen ions, water, carbonic acid and hydrogen sulfide.

The model also includes the formation of iron carbonate and iron-sulfide scales and their effect on the rate of general corrosion as a function of temperature and solution chemistry. The accuracy of the Anderko model has been verified by comparing calculated corrosion rates with laboratory data under conditions that may or may not be conducive to the formation of protective scales. Good agreement between the calculated and experimental corrosion rates has been obtained. This model incorporates the effects of temperature, pressure, solution composition, and flow velocity /20-22/.

Oddo Model

Protective films formed by the deposition of mineral scales have long been known to reduce or eliminate corrosion. FeCO₃ (or Fe₃O₄) layer deposition is accounted for in the de Waard and Milliams model; however calcite-scale deposits will also reduce or eliminate corrosion. Another scale-correction factor is introduced to account for the effects of calcium carbonate

scale on the overall corrosion rate. A correction factor, $F_{calcite}$, is defined. Local turbulence caused by a choke, a constriction in the pipe, an elbow, a drop, etc., will increase the scaling tendency locally. The transition zone between scaling with no corrosion and corrosion with no influence of the saturation of scaling materials is not clearly defined /23/.

Dayalan Model

This model consists of a computational procedure and a computer program to predict the corrosion rates of carbon-steel pipeline caused by CO₂-containing flowing fluids in oil and gas field conditions /24/. The computational procedure is based on a mechanistic model for CO₂ corrosion and was developed from basic principles. The model takes into account the CO₂ corrosion mechanism and the kinetics of electrochemical reactions, chemical equilibrium reactions, and mass transfer. A procedure that was developed to predict uniform CO₂ corrosion rates in the absence of scale was extended, using a mechanistic model of scale formation, to measure conditions where FeCO₃ layer formation occurs.

An iterative approach is used to predict the corrosion rate. Initially, the program calculates the corrosion rate assuming that there is no scale on the metal surface. The fraction of the metal surface that is covered by scale is set to zero, and the value of A_{Me} (the fraction of the metal surface that is bare) becomes 1 for this step /24/.

Pots Model

This mechanistic model predicts the CO₂ corrosion rate and the effects of fluid flow /25/. The model, also referred to as the Limiting Corrosion Rate (LCR) model, provides a theoretical upper limit for the corrosion rate based on the assumption that the rate-determining steps are the transport and production of protons and carbonic acid in the diffusion and reaction boundary layers.

Comparison with experimental data confirms that the LCR Pots model provides an upper flow limit. For flow velocities below 3 m/s under non-scaling conditions, there is reasonable agreement with single-phase flow experimental data and with pH values controlled by the partial pressure of CO₂. Inclusion of the charge-transfer kinetics provides a way to get

agreement at higher flow velocities. For flow velocities up to 1 m/s, corrosion rates predicted by the model agree with that predicted by the de Waard-Milliams nomogram /25/.

SSH Model

The SSH model is a worst-case scenario model, derived mainly from laboratory data below 100° C and from a combination of laboratory and field data at temperatures above 100° C /26/.

Adam Model

Adam's model, developed from the operating conditions of condensate wells, can be used to predict corrosion rates in gas condensate wells based on operating conditions, temperatures, and flow rates /27/.

Nyborg Model

Nyborg integrated the 1993 and 1995 versions of the de Waard Milliams models with a commonly used three-phase fluid-flow model. The temperature, pressure and liquid flow velocity profiles derived from this fluid-flow model are used to calculate CO₂ partial pressure, pH, and corrosion rate profiles along the pipeline /28-30/.

ELECTROCHEMICAL MODELS

The penetration of a pipe wall by a pit is a process that consists of three stages:

- 1. Formation of a passive layer on the steel surface;
- 2. Initiation of pits at localized regions on the steel surface where film breakdown occurs; and
- 3. Pit propagation and eventual penetration of the pipe wall.

Since electrochemical reactions are involved in all three stages, each phase of pitting corrosion can be modelled using electrochemical principles.

Passivity Models

Passive films generally form as bi-layers, with a compact layer adjacent to the metal and an outer layer comprised of a precipitated phase. They may incorporate anions and/or cations from the solution (in this case a salt film). Since passivity is still observed in the absence of the outer salt film, it is attributed to the compact layer. Porous salt films are often unstable, and are nearly impossible to study by *ex-situ* methods. Although salt films can have a dramatic effect on the passive film properties, electrochemical modelling assumptions have not been critically applied.

Several models for passive films on metals are reviewed in this paper. Validation of experimental results for each of these models, however, has not been consistent. Despite the fact that passive films on metals play a vital role in pitting corrosion, little systematic research has been undertaken to correlate the pitting susceptibility of carbon steel and the quality of the passive film on its surface.

Mott Model

Mott proposed the earliest models used to examine the growth kinetics of the passive film /31/. This model assumes that:

- Layer growth is due to the transport of metal cations across the oxide layer to the film/solution interface where they react with the electrolyte.
- The penetration of cations through the layer is assisted by the high electric field strength that is assumed to exist within the oxide.
- The field strength is constant throughout the layer.
- There is no potential drop across the layer.
- The rate-limiting step (RLS) for the layer growth is the emission of metal cations from metal into the layer at the metal/layer interface.

Mott-Cabrera modified the above place-exchange model with the following assumptions:

- Anion diffusion is responsible for layer growth.
- The RLS is the emission of an anion from the environment into the layer at the layer/environment interface.
- The field strength in the layer is independent of thickness.
- The activation energy of the RLS increases linearly with thickness.

Griffin Model

Griffin /32/ developed a simple kinetic model to relate the experimentally measurable features to the microscopic rate parameters of the passivation process, with the following assumptions:

- The oxidative hydrolysis of surface metal atoms produces adsorbed cations, and these cations dissolve away from the electrode surface.
- Passivation occurs when the rate of cation dissolution decreases as the cation coverage increases. The process occurs due to the stabilizing influence of the oxide lattice bond formation.
- The only feature that distinguishes an isolated adsorbed cation from a cation in the oxide layer is the presence of a full complement of nearestneighbour cations.

Using the results from cyclic voltammetric experiments, the Griffin model can be used to determine the factors that stabilize the passive layer on a metal surface.

Fleischmann Model

Defining passivation as the consequence of an ordered monomolecular two-dimensional film of a definite chemical phase, Fleischmann /33/ proposed the following:

- Using potentiostats suitable for measuring at high frequencies, measurements of the kinetics at constant potential will yield valuable information about the initial stages of passivation.
- Kinetics of growth can be obtained by considering that passivating centres of monomolecular height grow two-dimensionally on electrodes.
- The passivating centres are cylindrical in shape.
- If the nuclei are distributed over the surface in a completely random manner, an allowance for all possible forms of overlap between growing centres is made.

With the Fleischmann model, the rate constants for the nucleation of the passivation layers and their growth can be calculated using chronoamperometric (current-time curves) experiments conducted in the millivolt region.

Sato Model

In the Sato model /34/, an anodic growth rate of Fe is assumed to result from a process in which the activation energy increases linearly with thickness. It is also assumed that the oxide is an ordered Fe₃O₄ - Fe₂O₃ and that the rate can be calculated using concentrations, activation energies, and potential gradients.

According to this model:

- The film is a face-centred cubic lattice with an oxygen lattice parameter between 4.2 and 4.16. The potential of this system is equal to the sum of all the potential differences that exist between the metal and the solution.
- Under the steady growth region, equivalent numbers of iron and oxygen ions are transferred from the metal and solution phases into the oxide.

Based on these assumptions, the authors experimentally derived a rate equation that is of the same form as the kinetic equation. The Sato model can use data from both potentiostatic and galvanostatic experiments to calculate thermodynamic parameters including entropy and enthalpy of passive film formation.

Sarosala Model

The Sarosala model /35/ is based on Devillier's theory /36/, which states that:

- A solid insulating film of constant thickness, d_o, spreads over the electrode from random nuclei;
- The resistance of the layer-pore interface determines the rate of reaction; and
- The rate of reaction depends on the resistance of the electrolyte in the 'pores'.

This model takes into account both the intrinsic conductivity of the surface layer and its possible thickening by ionic transport through the material. Using fast-sweep cyclic voltammograms, both the thickness of the passivating layer and the degree of surface coverage can be determined.

Macdonald Model

Macdonald /37/ advanced a "point defect" model (PDM) to explain the growth, breakdown, and impedance characteristics of passive films on metal

surfaces. The most important assumptions of this model are:

- Whenever the external potential, V_{ext}, is more noble than the passivation potential, a continuous passive film will form on the surface of a metal.
- A passive film is assumed to be an oxide of composition M_{OX/2}. The
 passivation potential, E_{pass}, is the lowest potential at which the metal can
 be covered by an oxide film, which restricts the dissolution current.
- A passive film contains a high concentration of point defects, metal vacancy, electrons, and holes.
- Passive films are characterized by high electrical fields (10⁶ V/cm) and are assumed to be of the same order as that required for dielectric breakdown.
- Field strength is a function of the chemical and electrical characteristics of the film and is, therefore, independent of thickness, even under potentiostatic conditions.
- Electrons and electron holes in the film matrix are in their equilibrium states, and the electrochemical reactions involving electrons (or electron holes) are rate-controlled at either the metal/film or the film/solution interface.
- For those processes that involve metal and oxide vacancies, the ratecontrolling step is assumed to be transport of the vacancies across the film.

Using the Macdonald model and current-time plots, parameters that describe the dependencies of the potential drop across the barrier film/environment interface on the applied voltage and pH, and kinetic parameters for dissolution of the film can be calculated. These calculations require that many assumptions be made regarding the various constants described in the model.

Ambrose Model

Another important and practical consideration is 'repassivation,' which describes events that follow the rupture of a passive film /38/.

According to the Ambrose model:

- The repassivation process involves film coverage as well as anodic metal dissolution.
- The rate of coverage of the exposed metal determines the morphology of the corrosion attack.

- Low film coverage rates lead to the large active metal dissolution areas that are characteristic of pitting.
- The partition of the anodic current transient (into coverage and metal dissolution components) becomes important in the presence of large active metal dissolution areas.
- Immediately after the mechanical passive film rupture, the penetration rates of localized corrosion depends on the kinetics of repassivation.

Ambrose also showed that a powerful tool to distinguish between the soluble and insoluble reaction products of the repassivation process is the rotating ring-disc electrode.

Nucleation Models

There is much current debate concerning the initial steps of pitting corrosion. The *a priori* approach emphasizes the inherent microscopic defects such as inclusions, grain boundaries, and scratches on the metal surface. The *a posteriori* approach emphasizes the non-uniformity that becomes visible on the metal surface after a passive metal is placed in a corrosive media /39/.

The *a priori* approach assumes that heterogeneity is present on the passive metal, while the *a posteriori* approach assumes that an induced heterogeneity is present at the interface between the passive metal and the corrosive media.

In a posteriori assumptions, stochastic or fluctuation processes are thought to initiate pitting. Certainly, pit-initiation experiments seem to be subject to a much larger degree of experimental variation than other electrochemical experiments. The origin of this variation, however, is still open to discussion. Both the stochastic and deterministic approaches have value, and they are certainly not mutually exclusive.

Okada Model

The Okada /40/ model describes a passive metal in a corrosive environment where aggressive ions are transported and adsorbed through the passive film with spatial fluctuations. According to this model:

 During the initial stage, metal ions dissolve uniformly through the passive film, and the passage of the current transports halide ions by electromigration; the ions are then absorbed on the surface of the passive film.

- If the transport is perturbed resulting in a concentration of aggressive ions
 on the passive film surface, the dissolution rate changes locally causing
 variations in the ion flux.
- The system becomes unstable and, if the perturbation increases with time, promotes local destruction of the passive film.
- If the perturbation decreases, however, the passive metal dissolves uniformly, and no pits appear.
- Increases or decreases in the disturbance determine the possibility of pit nucleation. Thus, the pit initiation process is considered a probability event.

This model describes the critical wavelengths $[(\lambda)_c]$ for perturbation, where any disturbance in the solution accelerates the local dissolution of the passive film. A rough estimate of the wavelength of perturbation (that is, the point where instability sets in) can be made for typical values of parameters. The Okada model shows a clear distinction between those processes that lead to pit nucleation and those that do not.

By determining the potential developed as a function of chloride ions, we can calculate α_a – the transfer coefficient for conduction in the passive layer.

Shibata Model

Shibata /41/ considered pit generation events to be stochastic and analyzed it using a series or parallel combination of elemental-birth stochastic processes. The equations for survival probability, P, and time for pit generation, were formulated for each model, and the corresponding curves between ln(P) and time were also obtained. To determine which of the Shibata models to use, the distribution of the time for pit generation must be fitted to a specific model by numerical or graphic simulation.

Using the approach required by this model, the analysis of induction time for generation of pits may help to determine the dependency of the parameters responsible for pit initiation on the thickness and other properties of the passivating film.

Sharland Model

Sharland /42/ pointed out that assumptions made from a random pitinitiation experiment are not necessarily valid and that, therefore, the underlying mechanisms governing random pit initiation are not necessarily resolved. In this model, he investigated the nature of these underlying corrosion mechanisms.

According to the Sharland model:

- The process of pit initiation is deterministic, that is, the process can be described by a set of well-behaved differential equations.
- The long-term behaviour of the system is governed by a strange attractor, leading to the chaotic behaviour of the direct measures of the system.
- This attractor is embedded in a phase space of small dimension, that is, the system could be modelled by a small set of differential equations.
- This model does not indicate which variables govern the system.

Sharland claimed that, with a little physical insight into the problem, it may be possible to construct a deterministic model of the pit-initiation process /16/ if the factors leading to chaotic behaviour are understood.

Baroux Model

The Baroux /43/ model analyzes corrosion in two stages:

- The first stage of pit initiation the nucleation process leads to local breakdown of the passive layer resulting in direct contact between the base metal and the corrosive solution. The current increases markedly, and part of the dissolved metallic cations are hydrolysed, resulting in a local acidification. If this dissolution current is high enough to maintain a sufficient acidity despite the cation dissolution towards the bulk solution, the pit nuclei cannot repassivate, and a stable pit is generated. Thus, the pit nucleation process is described as a deterministic process characterized by an incubation time.
- The second stage of pit initiation namely the stabilization process is considered as probabilistic in nature and is characterized by a pitting probability. In other words, it is assumed that the incubation process does not necessarily lead to pit nucleation, but rather to a sensitized state from which a pit can occur.

The Baroux model can be used to determine the pit-generation rate, which can then be used to characterize steel in different environments.

Salvarezza Model

In the Salvarezza model /44/, the rate of birth and growth of a pit is

defined in terms of the rate of conversion of a surface site into a pitnucleation centre, while the rate of death is defined in terms of the probability of a pit dying.

According to the Salvarezza model:

- When the current exceeds a given value, the system becomes irreversible, and stable pits are formed.
- The pit-initiation process can be considered as stochastic or deterministic, depending on the time and potential duration of the experiment.
- The centres of pit nucleation are strongly dependent on the properties of the passivation layer and the presence of inclusions at that point.

This model can be used to determine the frequency of nucleation and the probability of pit death.

Hebert Model

The Hebert model /45/ is based on the hypothesis that:

- For metal immersed in a dilute sodium-chloride solution, initiation occurs
 when the concentration of dissolved metal exceeds a minimum critical
 value that can be determined experimentally.
- Only the period prior to the passivity breakdown is considered since, after this, many of the assumptions made are no longer valid.
- The system is solved numerically using a technique that linearizes the non-linear terms about a trial solution.
- Iteration is performed until convergence is reached.

Although this model was primarily developed to measure the crevice corrosion of aluminum, the general nature of the model may make it applicable to other types of localized corrosion as well as other systems. The complex mathematical calculations, however, require utilisation of modern computer power.

Williams Model

The Williams model /46/ is based on the following assumptions:

- The initiation of internal pitting corrosion requires the production and persistence of gradients of acidity and electrode potential on the surface roughness scale of the specimen.
- Fluctuations in the gradients, leading to the birth and death of events,

could arise because of fluctuations in the boundary layer in the liquid at the metal surface.

- A pit becomes stable when its depth significantly exceeds the thickness of the solution boundary layer.
- The solution boundary layer has two parts, one part being defined by the roughness of the surface, and the other by the hydrodynamic boundary layer.
- Local acidification would arise as a result of the hydrolysis of metal ions in the solution formed as a result of the slow dissolution of the passive metal.
- This passive metal-dissolution current could be considered variable over the surface because of inhomogeneities in the alloy composition or because of inclusions.
- A critical local solution composition can be defined, in terms of pH, for the initiation of pitting corrosion.
- The nucleation rate is determined by the time required to establish this critical local pH.

According to this model, the initiation of pitting corrosion is caused by the production and persistence of gradients of acidity and electrode potential on the surface roughness scale of the metal. The observed fluctuations are related to fluctuations in the hydrodynamic boundary-layer thickness. A pit becomes stable only when it exceeds a critical depth related to the surface roughness.

The Williams model can be used to determine the frequency of nucleation and the probability of pit death.

Bertocci Model

In the Bertocci model /47/ the current transients observed are assumed to indicate that the passive film has locally broken, causing anodic oxidation of the exposed metal, part of which forms a new passive film and part of which dissolves. The passive film is then weaker and more susceptible to further breaks, at least for a limited time, after which the breakdown rate probability returns to the initial value. The kinetics of repassivation may be temporarily slower, since some local acidification of the solution at the breakdown site may have occurred because of oxide precipitation.

According to Bertocci, the breakdown probability depends on the

intensity and is assumed after a breakdown to increase by an amount proportional to the electric charge passed, multiplied by a weighting factor that decreases monotonically with the time elapsed.

This stochastic model can reveal qualitative information regarding the probability of passive layer breakdown.

Oldfield-Sutton Model

Oldfield-Sutton /48/ developed a deterministic approach of characterizing localized corrosion. This model has been tested quite widely and forms the basis for many models developed later. The central theme of this model is the development a critical crevice solution (CCS), which is defined in terms of pH and chloride concentration. The permanent breakdown of the passive film and the onset of rapid corrosion occur only beyond the CCS.

In this model, the onset of crevice corrosion is treated as four-stage process:

- The environment becomes de-oxygenated due to restrictions on the transport of oxygen.
- The cathodic reaction switches to the outside of the crevice, and changes occur in the crevice solution.
- The crevice solution becomes sufficiently aggressive for the permanent breakdown of the passive film and the onset of rapid corrosion.
- The crevice begins to propagate.

The Oldfield-Sutton model is developed for stainless steels, but the theoretical treatment can be applied to other metals including carbon steel.

Xu Model

The basic approach of the Xu model /49/ is that the electric field varies through the surface layer thickness and between concave and convex regions. For an idealized single concave roughness, the electric field within the film may be calculated by solving a boundary value problem. For a non-active pit, the whole pit wall is in the passive state. Breakdown occurs when the electrostatic pressure at the film/solution interface of the local site exceeds the compressive film strength.

Adsorption of aggressive ions, such as chloride ions, reduces the surface energy at the film/electrolyte interface. The higher the concentration of the aggressive ion in the solution, the higher its surface coverage ratio due to

adsorption and thus the lower the surface energy. At high concentrations of aggressive ions, the electrostatic pressure at the concave sites will more easily reach the value required for local breakdown to occur. Thus, aggressive ions are required for pit initiation.

Using a boundary variation and a trial-and-error technique /50/, the current and potential distribution along the pit depth can be calculated to determine the depth of the pit that is active, and hence susceptible to propagation.

Lillard Model

Lillard /51/ developed a model based on the concepts of the Oldfield-Sutton /48/ model (effects of mass transport) and the Xu model /49/ (ohmic control). The Lillard model analyzes the factors that contribute to the initiation and propagation of crevice corrosion using SPICE (simulation program with integrated circuit emphasis). By arbitrarily fixing the values of the criteria required to initiate crevice corrosion, the model generates current and potential distributions within the crevice incipient to the initiation of crevice corrosion.

These basic criteria of the model are:

- A critical crevice solution pH must be developed.
- A geometric solution resistance down the length of the crevice is necessary so that E_{crevice} < E_{pass} and a sufficiently high dissolution rate exists at the active site.
- The driving force of this model is represented by E_{cell}, which is the algebraic sum of anodic, cathodic, and ohmic overpotential.
- Different positions inside the crevice are characterized by different resistances.
- Four resistances are defined:
 - R_{pass} resistance associated with the passive dissolution inside the crevice,
 - R_{act} resistance associated with the active site inside the crevice,
 - R_{ni} potential dependent resistances in the active region, and
 - R_p polarization resistance.
- During calculations, the positions of these resistances are suitably altered so that the model converges for the predetermined basic criteria.

Though this model was primarily developed to monitor crevice corrosion, its basic concepts can also be applied for the pitting corrosion of other metals

and alloys. The crevice depths (which are susceptible to further corrosion) can be calculated using the primary knowledge of critical-crevice solution (pH) and active dissolution kinetics. However, the accuracy of the model's prediction of the time taken for a crevice to occur may be less than the actual time taken, because of the various predetermined and arbitrary values used in the model.

The important outputs of this model are: critical depth as a function of crevice gap, and critical gap/depth combinations as a function of crevice initiation.

Bardwell Model

In this model, iron is protected from pitting by a halide-containing solution. The surface is covered by a passive layer the thickness of which is greater than the critical thickness /52/.

In this model:

- Pitting initiates in the presence of halide ion only if the passive layer reaches a certain critical thickness.
- The critical state of the layer growth corresponds to a critical oxide thickness, as opposed to critical oxide composition.

Dawson Model

In the Dawson model, pit initiation is considered an electro-crystallization process with chloride ions playing a major role in pit formation, with the adsorbed intermediate produced on the metal surface /53/.

According to this model:

- Pit growth and arrest are essentially seen as a kinetic competition between
 the formation of non-passivating species [MOMOHCl]_{ad} and
 [MOMHCl]_{ad}, and passivating species [MOOH]_{ad} and [MOMOH]_{ad}.
 Passive film rupture is considered to be a normal occurrence that
 increases in intensity with increasing potential and/or aggressive ion
 concentration.
- The electrostatic model involving chloride-ion adsorption on the outer film is, therefore, considered.
- Progression from the initial film rupture to pit propagation is also controlled by the potential, chloride ion and diffusion, within both the crack and the growing pit.
- With increasing potential, the influence of adsorbed intermediates on the

metal-dissolution kinetics becomes increasingly important.

Hebert Model

According to Hebert, before a crevice is formed, the metal surface corrodes uniformly at a low rate.

The basic criteria of this model are:

- Since corrosion within the crevice progresses, metal species are concentrated in the crevice, and oxygen is depleted from it /54/.
- When the cathodic reactant has been removed from the crevice, a net anodic reaction within the crevice is balanced by oxygen reduction on the metal outside the crevice.
- Chloride ions migrate into the crevice in response to the potential gradient that now exists.
- The hydrolysis of metal ions causes acidification of the crevice.
- Initiation occurs when the concentration of dissolved metal exceeds a certain minimum critical value.

McCafferty Model

This competitive adsorption model claims that pitting is inhibited when aggressive ions (CI) and inhibitive ions compete for sites on the metal surface /55/. If the ratio of the surface coverage of aggressive to inhibitive ions exceeds a certain critical value ($\theta_{\text{,crit}}$), then breakdown of passivity occurs accompanied by pitting.

MacDonald Model

MacDonald developed a point-defect model /56/ to investigate the steadystate properties of the passive films that form on metals and alloys in aqueous environments. He further developed a deterministic model /57/ to describe the statistical nature of passive film breakdown and pit nucleation, based on the following criteria:

- A solute-vacancy interaction model (SV) is needed to account for the
 effects of minor alloying elements, such as Mo and W, on the pitting
 resistance of iron-based alloys.
- The point-defect model upon which the SV is based proposes that
 passivity breakdown occurs because of an enhanced flux of cation
 vacancies from the film/solution interface to the metal/film interface. The
 excess vacancies arriving at the interface between the metal and the film

cannot be absorbed into the metal at a sufficiently high rate.

- Accordingly, the vacancies accumulate to form a vacancy condensate at the metal/film interface, which then grows to a critical size.
- The film then collapses locally to form a pit that will continue to grow if conditions are not conducive for repassivation.

The distribution in breakdown probability is sensitive to the mean cation vacancy diffusivity, but not to the standard deviation. As the distribution is shifted to more positive values, the cation vacancy diffusivity becomes smaller, indicating that the passive film becomes more resistant to breakdown. Increasing halide activity and decreasing pH are predicted to shift the distributions in breakdown probability to more negative values, thereby rendering the passive films more susceptible to breakdown.

The MacDonald model can be used to predict the steady-state thickness of the passive layer and its breakdown.

Propagation Models

The final stage of pitting corrosion is the formation and continuous propagation of stable pits. In propagation models, the growth of pits is treated as deterministic. When the pit becomes sufficiently large, the conditions and processes taking place are closely related to those occurring in crevice corrosion.

Nagatani Model

Nagatani /58/ developed a model based on the following considerations:

- A pit starts to grow from a single defect on the metal surface.
- During pitting corrosion, anionic species diffuse toward the metal surface.
- After diffusing anions arrive at the metal surface, the metal dissolves into solution because of the hydrolysis of metal ions; this process is controlled by the diffusion of anions.
- Concentration of the diffusing anions satisfies the Laplace equation under the quasi-stationary approximation.

Using a three-dimensional computer simulation for pit formation, the geometry of a pit can be obtained.

Matamala Model

Matamala /59/ empirically created an analytical expression using variables such as pH, chloride-ion concentration and temperature :

$$E_p = 2570 - 5.81T + 0.07 T pH - 0.49T log[Cl],$$

where E_p is the passivation potential. Cl^- is the chloride-ion concentration. These expressions are very specific and do not convert easily to other systems without further experimental verification.

Smyrl Model

In an attempt to analyze the effects of minor components on the propagation of a crack, Smyrl /60/ developed a model that determines the potential distribution in a crack from the distribution of the flux. The important assumptions of the Smyrl model are:

- The crack is wedge-shaped with a geometrically sharp tip, and it extends through the thickness of the material.
- The coordinate system moves with the crack tip, so that the sides of the crack appear to move with the velocity away from the tip.
- The flow pattern of the liquid is determined by the fluid mechanics of the system.
- The velocity profiles are not changed by the mass-transfer processes;
- At greater distances from the crack tip, inertial and pressure forces determine the fluidflow characteristics, except near the crack walls where viscous forces are also important.
- Migration effects are not important under these conditions.

The potential distribution along the pit length can be determined from the measurable parameters including velocity, mass-transfer coefficient, and bulk concentrations of the reactants. For the diffusion layer region, the integration could be carried out directly to obtain an analytic result. Tedious calculations are the main drawback of this model. Nevertheless, it can provide valuable information on potential differences from comparatively easily measurable quantities.

The model further predicts that the potential difference between two points would be directly proportional to the bulk concentration or the reactant, and inversely proportional to the square of the pit width. Hence, an approximate estimate of potential difference between two points can be obtained from the measured pit width.

Fan Model

Fan /61/ developed a very simple model to correlate the potential drop with the pit-propagation rate. It is based on the following considerations:

- Corrosion potential shifts in the noble direction when active dissolution occurs.
- Current passing through the passive film is equivalent to the amount of passive layer dissolution.
- The pit area is used as the corroded surface area.
- Any increase in exposed surface due to growth of pits is ignored.

Though the model is qualitative, information on pit propagation can be obtained from the potential change.

Molo Model

Molo /62/ used a stochastic principle to measure pit growth. This model applies to a process initiated at reacting inclusions in the metal and determines the development of quasi-hemispherical pits.

The model is based on the following main hypotheses:

- Pits are initiated at reacting inclusions on the metal surface. The mean number of inclusions per unit of area, <n₀>, depends on the material.
- Pit-initiation events are randomly distributed in time, and the distribution, (λ)_o, depends on the corrosion conditions.
- The pit-surface concentration is sufficiently low to make it possible to ignore the overlapping of pits.
- The growth rate of each pit, $(\lambda)_k$, depends on the area of the active interface.
- Pits are unstable when they are nucleated and become stable only after they have grown beyond a critical volume, V_c, from which a critical time, t_c, can be derived.

The Molo model can be used to determine the distribution of pits and the critical volume required for pits to stabilize.

Tester Model

Tester /63/ developed a simple model to distinguish between two distinct phases of pit growth.

According to this model:

- During the early period of dissolution, the electrode surface is flush with the surface of the cavity. A semi-infinite approach is used to model the diffusion process that causes the electrolyte concentration to increase at the metal surface.
- Once saturation of the dissolving cation species occurs at the metalsolution interface, after the initial period, a quasi steady-state period of diffusion control commences.

The time-dependent reactant depletion can be obtained from this model. These expressions may be approximate, but they can provide a reasonable basis for assessing the reactant concentration in a crack and the factors that can affect it. From the reactant depletion rate, the pit growth rate is determined.

Beck Model

Since the geometry and migration effects exert opposite and nearly equal influences on the dissolution rate, Beck's model assumes that they cancel each other out /64/. In this model, the depth of the pit can be determined as a function of time.

Ateya Model

Ateya /65/ proposed a model to determine the electrochemical conditions and the ongoing electrode reactions within cracks in metals during cathodic charging.

The Ateya model assumes the following:

- A narrow, deep slot with an outer surface is maintained at a large negative potential so that the only reaction taking place at the outer surface is hydrogen evolution. The cross section of the slot is a rectangle with dimensions A and B, and depth L, such that A << L and A << B, in which case the reaction can be considered to occur only on the outer surface and on the side walls.
- A more precise condition for validity of the equations is X >> A, where X is the characteristic distance defined.

- It is assumed that mass transfer in the electrolyte takes place by molecular diffusion and ionic migration.
- The electrolyte is a simple acid that dissociates completely to give monovalent ions.

This model can be used to calculate the pit growth rate.

Ben Rais Model

In the absence of convection, Ben Rais et al. /66/ obtained an analytical solution to calculate the current delivered as a function of time from the corroding sample.

The four main approximations of this model are:

- Diffusion and migration effects are calculated assuming the solution is very dilute.
- Saturation at the bottom of the pit is considered without taking into account the effects of supersaturation, pH variation and ionic strength.
- Metal hydrolysis is neglected.
- The curve expressing the variation of the corroded area as a function of time is heavily schematized.

Using Faraday's law, the pit growth rate can be calculated from the current.

Melville Model

Doig and Flewitt /67,68/ considered the variation of potential occurring down a stress corrosion crack, assuming Tafel kinetics. Melville /69/ extended Doig and Flewitt's analysis to examine the effect of an arbitrary relationship between the current and the potential at a crack tip to obtain analytic solutions for those conditions where the variation in potential is small. The potential drop in a pit can be determined by studying the electrochemical reactions.

Galvele Model

In a sequence of papers, Galvele /70-72/ constructed a complex model of pitting corrosion. In the first paper, assumptions from the Pickering model /50/ were used, but, instead of a single-charge transfer reaction, a more general expression was considered for the anodic reaction occurring inside

the pit.

The Galvele model assumes that:

- Dissolution takes place at the bottom of the pit, and no reaction takes
 place on the walls of the pit. In this way, a unidirectional pit model is
 obtained using a simple mathematical procedure.
- The pH of the bulk solution could have been given any value, but is given as a boundary condition. Hydrolysis equilibrium is very quickly reached.
- Aggressive anion salt acts as a supporting electrolyte for the ionic species.
- Modifications are made by considering full hydrolysis of the metal ions and the effects of ion migration and buffers. Contributions due to convection are ignored.
- The main reason for passivity breakdown at the initial stages of pit growth is localized acidification due to metal ion hydrolysis.
- The pitting potential is the critical point at which a minimum X·i value for pit initiation is reached, where X is the pit depth and i is the current density.

This model can be used to obtain the relationship between the concentration of chemical species and the product of pit depth (X) and current density (i).

Alkire Model

The important assumptions made in the Alkire /73/ model are:

- Metal dissolution is the only electrochemical reaction that occurs inside a pit.
- During dissolution, the metal surface is assumed to remain smooth and perpendicular to the side walls.
- During dissolution, the solubility of the metal salt is not exceeded, and therefore precipitation does not occur.
- Initially, the concentration within the pit is uniform prior to the application of power.
- At the base of the pit, the concentration gradient in the metal salt is proportional to the current flowing through the pit.
- As the metal dissolves, the pit becomes longer. For short-duration unsteady-state experiments, the elongation of the pit is less than 0.03% of the initial length, whereas for longer-duration steady-state experiments,

the variation in pit length during dissolution can be accounted for using Faraday's law.

This model can be used to determine conditions leading to the autocatalytic growth of pits.

CORROSION ENGINEERING MODELS

A corrosion engineer typically determines the risk caused by internal pitting corrosion from field operating conditions, from in-line inspection (ILI) data, and from on-line monitoring techniques.

Data provided by an oil production company were examined to determine if there was any correlation between pipeline failures and operating conditions. For each pipeline, the records consisted of monthly values for the average daily oil, water and gas production, and percentage water-oil ratio (water cut). Time series of these values were constructed backwards in time from the most recent. For those pipelines having gaps in the records, the time series was halted at the time of the first gap.

By including only those pipelines with records of at least 100 months, the data for 73 bare steel pipelines were analyzed. These pipelines included 67 well lines (seven of which had failed), three satellite lines (one of which had failed), and three transportation lines (one of which had failed). The outside diameter and wall thickness of these pipelines ranged from 60.3 to 168.3 mm and from 2.8 to 4.78 mm, respectively, with the most common dimensions being 88.9 mm and 3.96 mm.

The simplest step in finding a correlation was to determine if a distinction could be made between failed and non-failed lines with respect to simple flow variables. The explicit dependence of flow rate on the (inside) pipe diameter, d, was removed by calculating superficial flow velocities according to:

$$v_k = \frac{4Q_k}{\pi d^2} \tag{Eq. 1}$$

where Q_k is the volume flow rate of the fluid component k (and k = 0, w and g for oil, water and gas, respectively). The gas velocity, v_g , was calculated from

the gas production rate, which was expressed in m^3 /day at standard temperature and pressure. Since the actual temperatures and pressures of the fluids were not given in the database, the true gas volume could not be determined, so that ν_g is an approximation. If the pipeline pressures and temperatures were comparable, then the relative values of ν_g are correct.

To facilitate the comparison between failed and non-failed lines, the mean value, v_k , and standard deviation, σ_k , of v_k were calculated. Subscripts n and f denote non-failed and failed lines, respectively. For any difference between v_{kf} and v_{kn} to be significant, v_{kf} must be outside the limits defined by $v_{kn} \pm \sigma_{kn}$.

The data for the individual lines and for the average values can be summarized using the following factors: flow velocity, water cut, flow regime, pipe inclination, H₂S concentration and pressure.

Superficial Oil Velocity

Oil flow decreased with time for most failed lines, but, in all cases, $v_{of} < 0.025$ m/s at the time of failure. For one line, this represented an order-of-magnitude decrease from a peak velocity of 0.2 m/s. In Fig. 1, v_{of} is somewhat less than v_{on} , but during the entire period the difference was always less than σ_{on} .

Superficial Water Velocity

At the time of failure, v_{wf} always varied by an order of magnitude of more than 0.04 m/s to 0.9 m/s. Sudden substantial increases in v_{wf} occurred in two lines about 65 months before failure. These two lines are responsible for the increase in v_{wf} at -65 months, as shown in Fig. 1. The mean water velocity of the failed lines, v_{wf} , was somewhat higher than v_{wn} , but the difference was consistently less than σ_{wn} .

Superficial Gas Velocity

This quantity was calculated from the produced gas volume measured at standard temperature and pressure (STP) and is, therefore, very approximate. At failure, v_g , was <4 m/s for all nine lines, and one line exhibited very large fluctuations. As was the case for both liquid components, v_{gf} and v_{gn} differed by less than σ_{gn} .

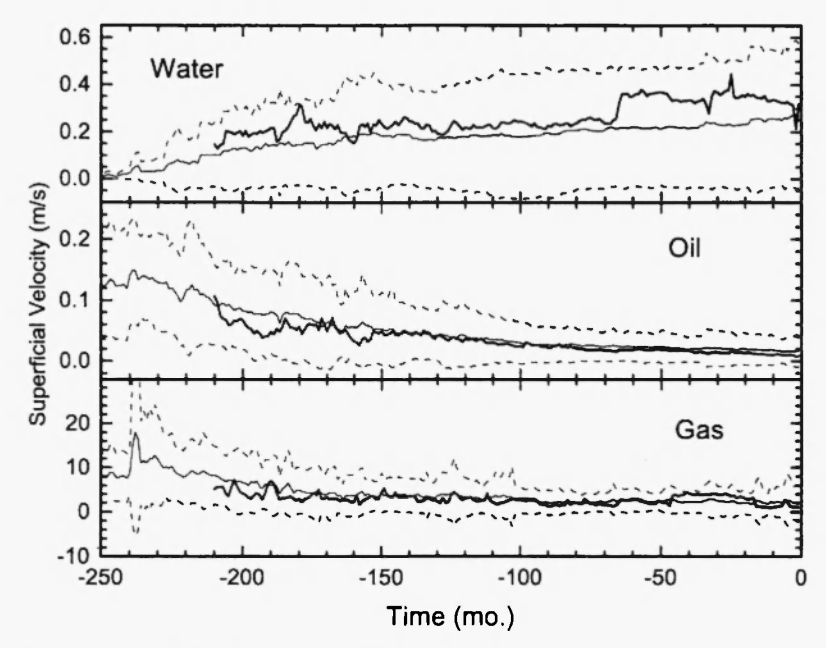


Fig. 1: Time dependence of the mean superficial oil, water, and gas velocities for failed (heavy line) and non-failed (light line) pipelines.

The dashed lines indicate the mean ± standard deviation for non-failed lines.

Water Cut

There was a wide variation in water cut among the failed lines. For two failed lines, the water cut exceeded 90% for 200 months, but for another failed line it was greater than 60% for less than 50 months. As shown in Fig. 2, the average water cut was somewhat higher for the failed lines than for the non-failed lines, but the difference was always less than the standard deviation.

Flow Regime

For multiphase flow, the aqueous-oil-gas interphases can take any one of an infinite number of possible forms. These forms are delineated into certain classes of interfacial distribution called flow regimes. The flow regimes depend on the inclination of the pipe (that is, vertical or horizontal), flow rate

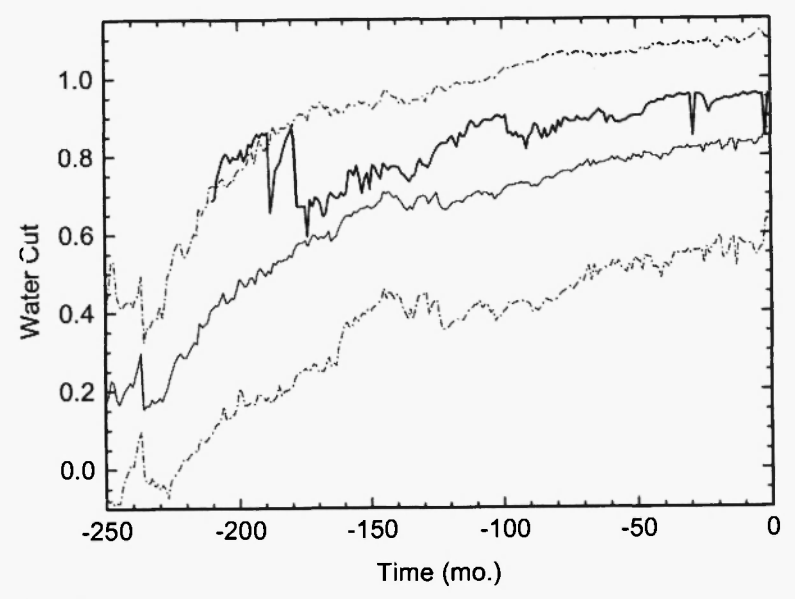


Fig. 2: Time dependence of the mean water cut for failed (heavy line) and non-failed (light line) pipelines. The dashed lines indicate the mean ± standard deviation for non-failed pipelines.

(based on production rate), and flow direction (that is, upward or downward). For horizontal pipes, bubbly, stratified, wavy, plug, slug, and annular flow regimes are possible /74-77/.

Figure 3 shows a plot of v_l against v_g for 69 lines (data for four non-failed lines with $v_g > 10$ m/s are not included in this figure). The velocities were calculated from the average flow rates for the most recent 12-month period. No distinction between failed and non-failed lines was noted, although there were no failures for lines with $v_g > 3.5$ m/s. Furthermore, if the transition from stratified to slug flow occurs at $v_l \approx 0.2$ m/s, then pipelines in both regimes failed.

Pipe Inclination

In Figs. 4, 5 and 6, the two-dimensional pipeline side elevations derived from pipeline and topographical surveys were compared with in-line inspection data to predict where corrosion would occur. No correlation could be established between pipeline elevation and internal pitting corrosion /78/.

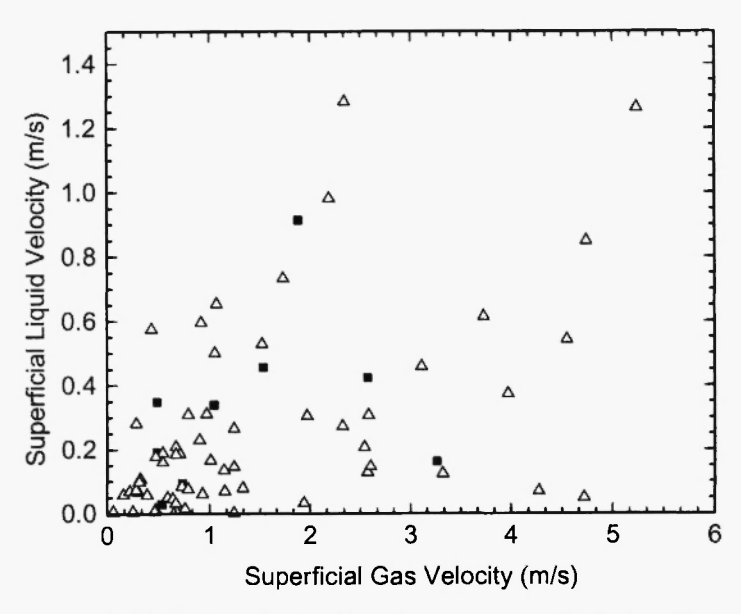


Fig. 3: Superficial liquid velocity plotted against superficial gas velocity for failed (squares) and non-failed (triangles) pipelines.

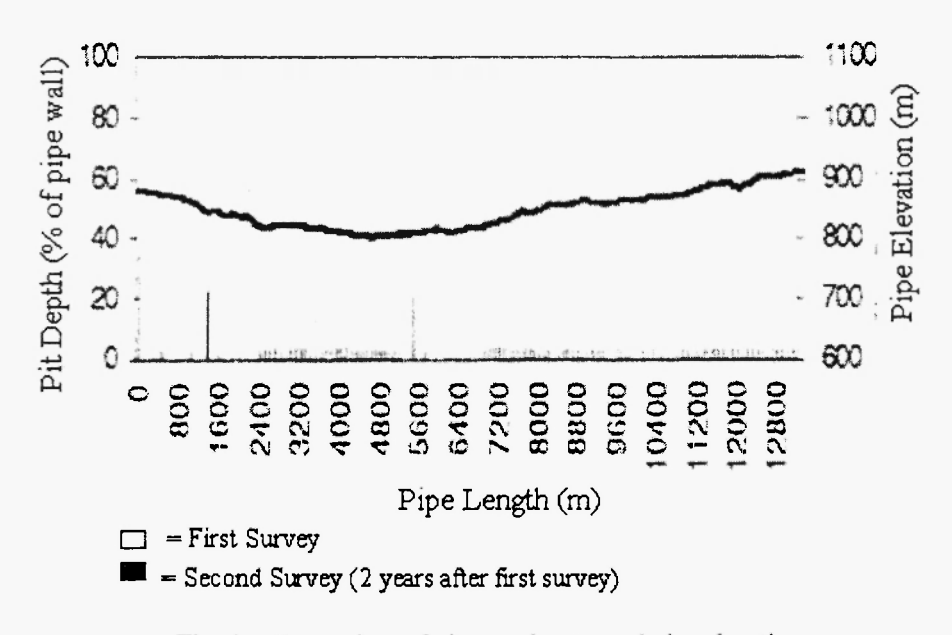


Fig. 4: Comparison of pit growth rates and pipe elevation.

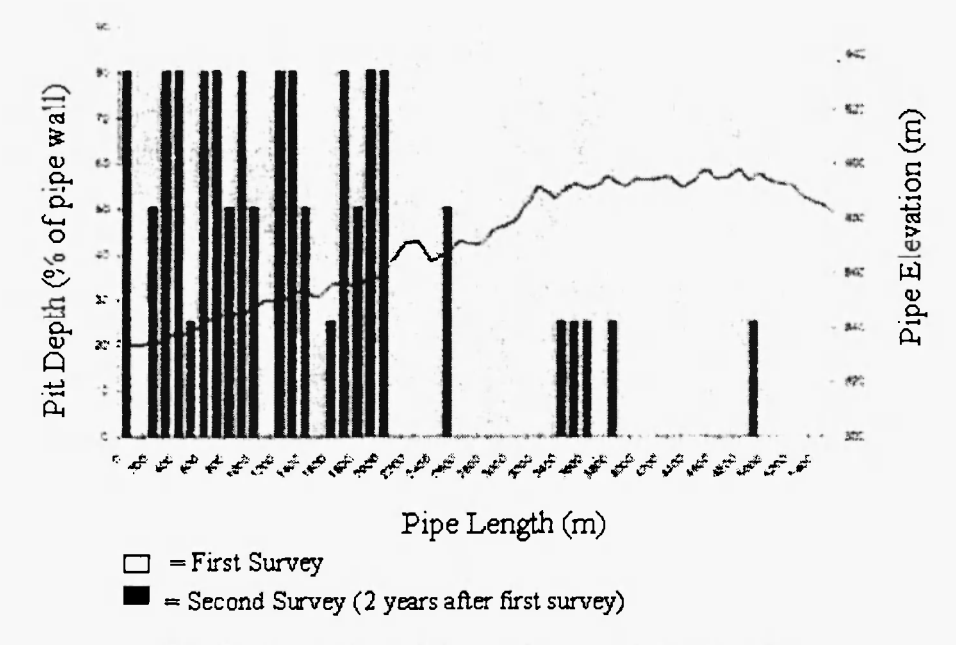


Fig. 5: Comparison of pit growth rates and pipe elevation.

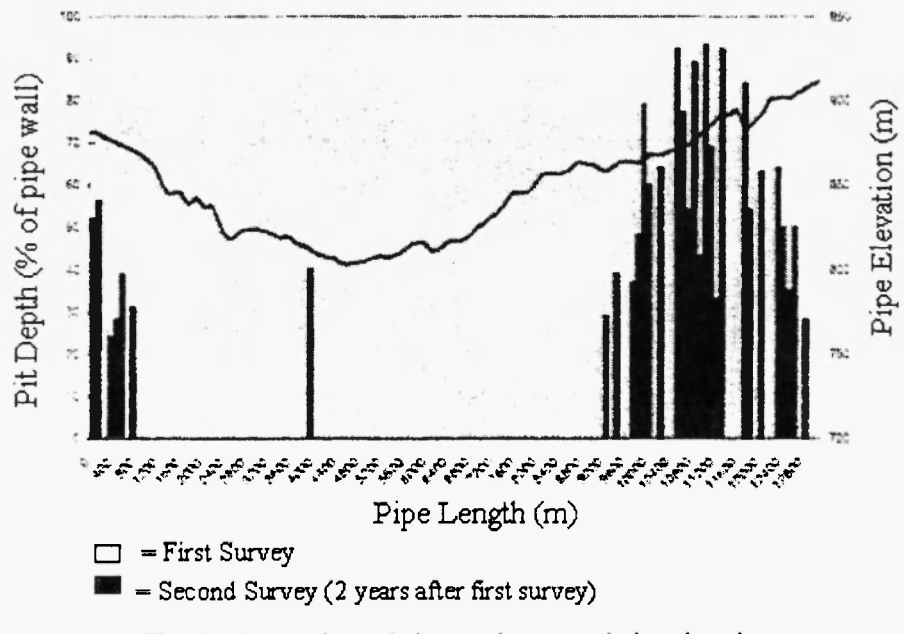


Fig. 6: Comparison of pit growth rates and pipe elevation.

H₂S Concentration /79/

Using different data from failed pipelines, the pit growth rate was calculated as:

Pit growth rate = Pipe thickness/(time of first failure – time of installation).

As shown in Fig. 7, the growth rates were plotted against the partial pressure of H_2S at the time of failure. No correlation between pit growth rate and partial pressure of H_2S could be established.

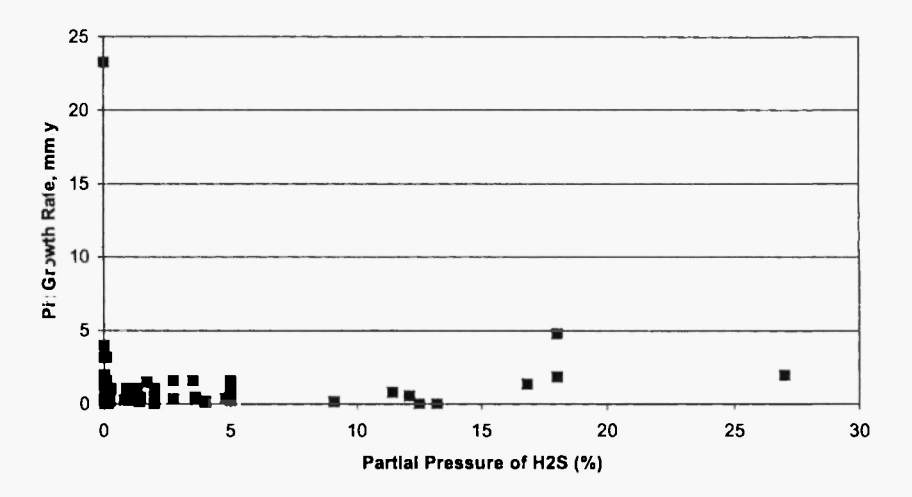


Fig. 7: % H₂S versus pit growth rate.

Pressure /76/

In Fig. 8, the pit growth rates (as determined in the H_2S concentration section) were plotted against normal operational pressure and, in Fig. 9, against maximum operational pressure. No correlation between pit growth rates and pressure could be established.

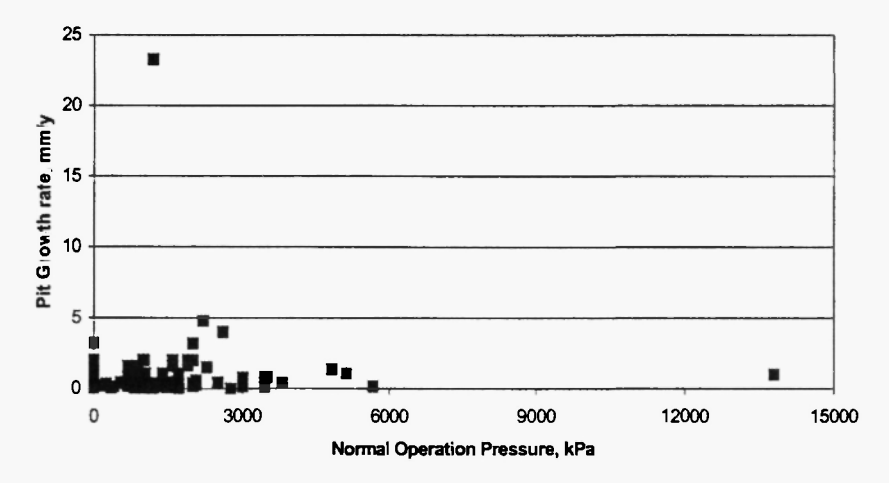


Fig. 8: Normal operation pressure versus pit growth rate.

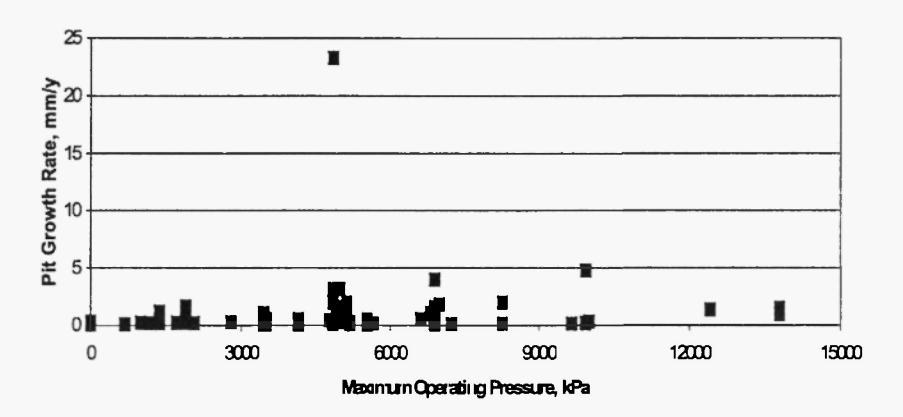


Fig. 9: Maximum operating pressure versus pit growth rate.

DISCUSSION

The ability of models to predict the risk of internal pitting corrosion can be summarized by assessing the answers to the following six key questions that can be obtained by using the models.

1. Does internal pitting corrosion pose a significant risk?

Almost all corrosion science models can answer this question, but the accuracy of the results is not guaranteed because the prediction is based on general corrosion rates not on pitting corrosion rate. Experiments to establish the corrosion science models outlined in this paper are clearly defined and are carefully performed under controlled conditions. The influence of the individual parameters is well understood. General corrosion rates leading to the formation of surface layers under the experimental conditions relevant to oil and gas pipeline conditions are readily available. As presented in Figs. 10-

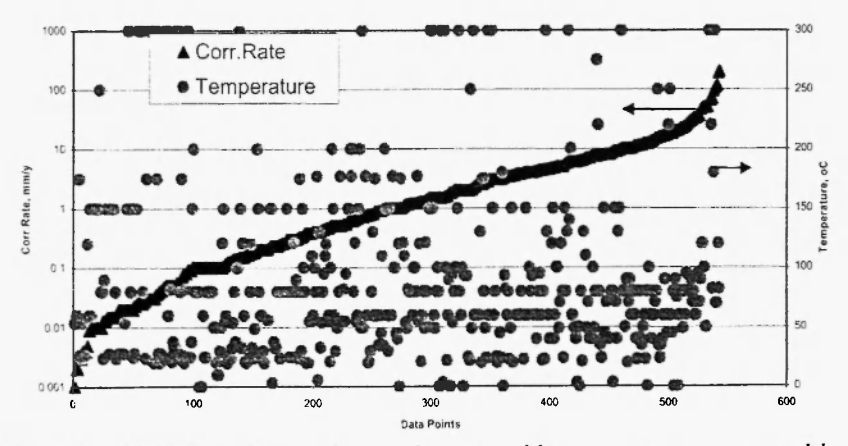


Fig. 10: Variation of general corrosion rate with temperature as reported in Reference from 80 to 160. (In addition results are also reported at 310, 454.4, 600, 635, and 700°C).

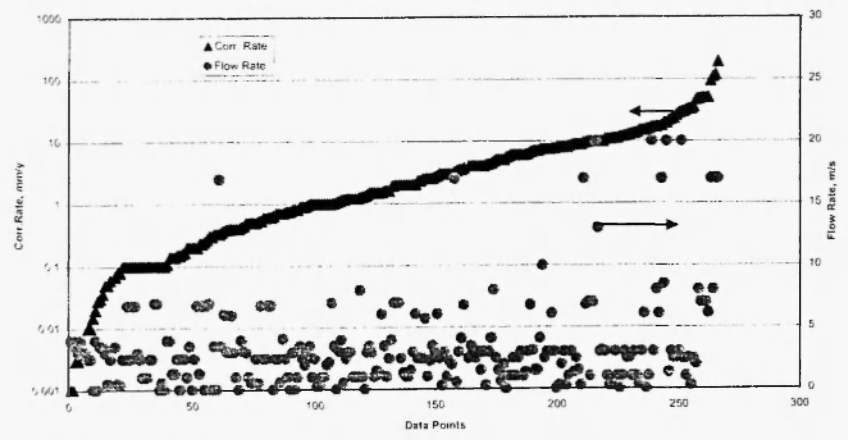


Fig. 11: Variation of general corrosion rate with flow rate as reported in References from 80 to 160.

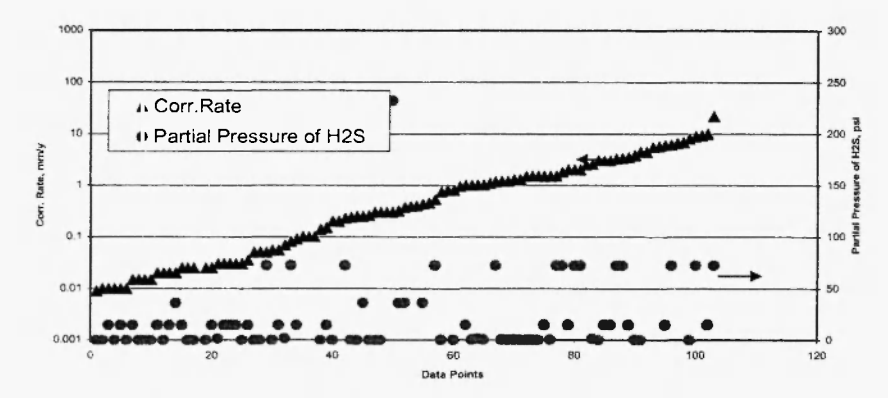


Fig. 12: Variation of general corrosion rate with partial pressure of H₂S as reported in References from 80 to 160. (In addition some results are also reported at 362.5, 870.3, 1000, and 10,000 psi)

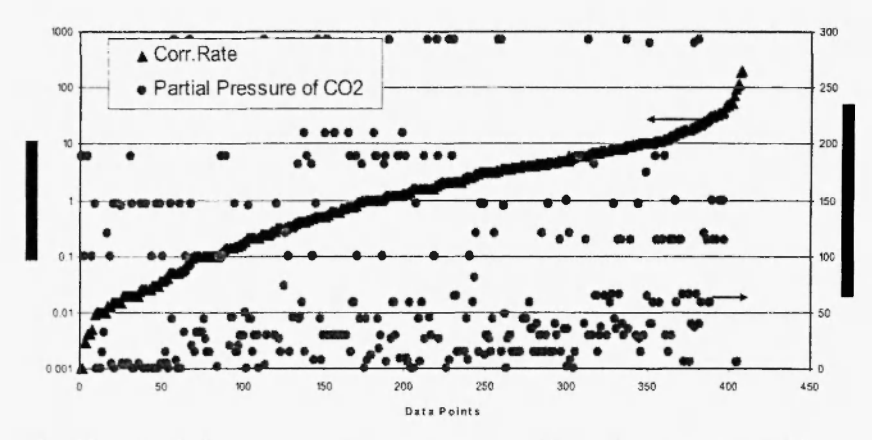


Fig. 13: Variation of general corrosion rate with partial pressure of CO₂ as reported in References from 80 to 160. (In addition of some results are also reported at 362, 435, 580, 725, 732, 800, 1000, and 2300 psi).

17 and Table 1, the results obtained can be influenced by various parameters /80-160/. As can be seen from the figures, the corrosion rates differed by 5 orders of magnitude for each set of parameters.

According to electrochemical models, internal corrosion becomes an issue if the passive layer becomes unstable. Since several passivation models are available, there are multiple outputs. To develop and verify a unified, reliable model, the predictions should be compared with the field data. From the

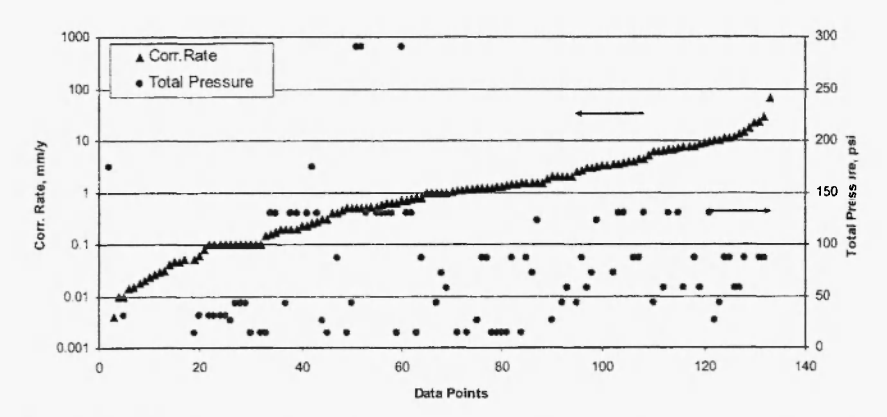


Fig. 14: Variation of general corrosion rate with total pressure as reported in References from 80 to 160. (In addition, some results are also reported at 1204, 1440, 1885, 2000, 2197 and 2901 psi).

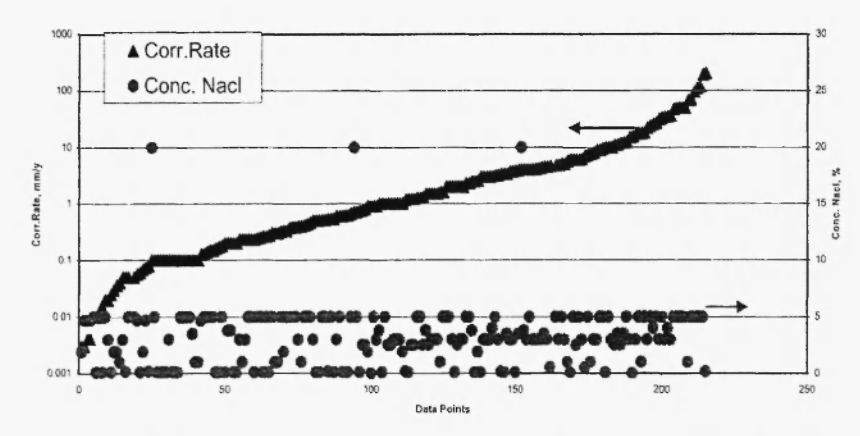


Fig. 15: Variation of general corrosion rate with concentration of NaCl as reported in References from 80 to 160.

comparison, a best result can then be selected.

Vast experience has been accumulated in the industry over 50 years of operation. In theory, a corrosion engineer could, based on operating conditions and data from monitoring techniques, predict whether internal pitting corrosion will be an issue.

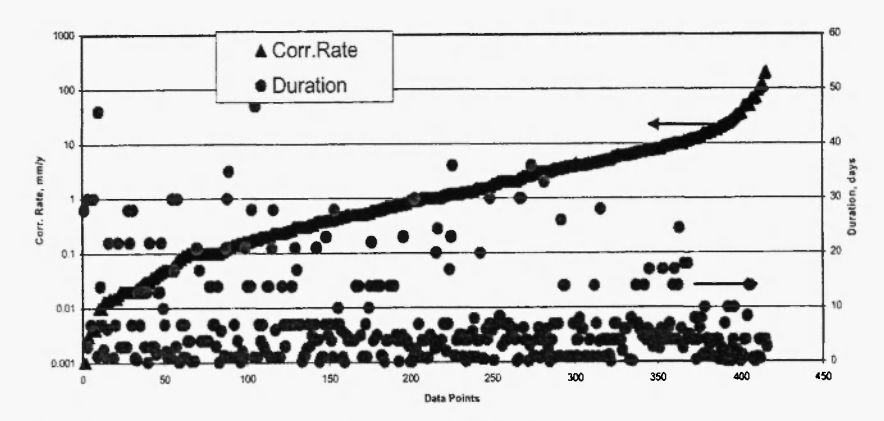


Fig. 16: Variation of general corrosion rate with duration as reported in References from 80 to 160.

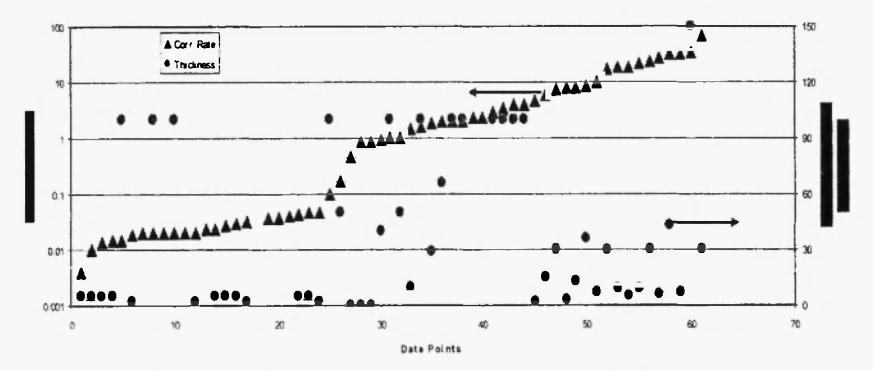


Fig. 17: Variation of general corrosion rate with thickness as reported in References from 80 to 160. (In addition some results are also reported at 160, 175, 500 and 900 μ m).

2. When, during operation, is a failure likely to occur?

Based on the general corrosion rates determined in the laboratory, this question can be answered, but again the accuracy of the results is not guaranteed because the corrosion science models deal only with one of the three aspects of pitting corrosion, i.e., surface-layer formation. The reasons for this include shorter duration of experiments (and hence the pit initiation and propagation are not observed) and disagreement between prediction of corrosion models derived from the same set of experiments.

 Table 1

 Compositions of surface layers formed in oil and gas pipelines /80-160/

Surface compositions	Number of references
FeCO ₃	121
FeCO ₃ , Fe ₃ C	12
FeS	21
FeCO ₃ , Fe ₃ O ₄	14
Fe ₃ C	24
FeCO ₃ , Fe ₃ O ₄ , Fe ₃ O ₂ , FeO	25
Fe ₃ O ₄	17
Fe ₃ O ₄ , α- Fe ₃ O ₂	15
FeCO ₃ , Fe(OH) ₂	18
FeCO ₃ , Cr(OH) ₃	13
Other (LiFe ₅ O ₈ , FeS ₂ , CaCO ₃ , Fe ₉ S ₈)	24

When stable pits are formed, that is when random nucleation and repassivation of the pits results in the formation of a few stable pits, they have the energy to grow continuously. At this time, internal pitting corrosion becomes an issue. Since several nucleation models are available, there are multiple outputs. To develop and verify a unified, reliable electrochemical model, the predictions should be compared with the field data. From this comparison, a best result can be selected.

The corrosion engineering approach has established threshold operating conditions when internal pitting corrosion becomes an issue. This rule-of-thumb approach has not always proven to be reliable.

3. Where in the pipeline is the failure likely to occur?

Corrosion science models have not been sufficiently developed to answer this question.

A stable pit, that is a pit beyond a certain depth, propagates autocatalytically at rates depending on the environment and on the size and shape of the pit. When the fastest growing pit reaches the depth of the wall thickness of the pipe, the first internal corrosion failure occurs. Since several pit propagation models are available, there are multiple outputs. To develop and verify a unified, reliable model, the predictions should be compared with the field data. From the comparison, a best result can then be selected.

Companies test, evaluate, and use many techniques to monitor pipeline reliability. Monitoring techniques can be broadly classified into: physical techniques, electrochemical techniques, non-intrusive techniques /161/, online monitoring techniques, off-line monitoring techniques, and new techniques. If the monitoring techniques are applied at appropriate locations, or if the ILI technique can be used, and if the operating parameters are accurately known, the location where the risk caused by internal corrosion has exceeded a pre-set limit can be determined.

4. What is the failure mechanism likely to be?

In the field, one of the main causes of pipeline failure is localized pitting corrosion, but none of the models mentioned can predict where this pitting corrosion will occur because the corrosion science models deal only with one (surface layer formation) of the three stages of pitting corrosion. Corrosion science models cannot accurately predict information on localized corrosion, because the duration of experiments conducted to develop the models is too short for localized corrosion to begin.

By integrating pit nucleation and propagation models, the mechanism by which the internal corrosion failure occurs in oil and gas pipelines can be developed. Laboratory experiments are required to adapt the constituent models to pipeline environments and to complete the knowledge required on pitting corrosion of oil and gas pipelines. The experiments must be carried out at pressures and temperatures similar to pipeline operating conditions.

Almost all failures are caused by localized corrosion in the form of isolated pitting. Depending on the monitoring or inspection techniques used, the size and shape of the pits could be determined and monitored.

5. Which operating parameters should be monitored to accurately predict the failure?

The corrosion science modelling approach is dynamic in nature. As more experimental data become available, the models can be updated. However, the number of parameters required to make an accurate prediction has not been established. None of the electrochemical models have been adapted to oil and gas pipeline operating conditions, because of the large number of parameters required to make the prediction (see Table 2).

Table 2

Number of parameters required for electrochemical models to predict internal pitting corrosion.

Pitting corrosion	Number of	Assumed	Number of			
	inputs	constants	outputs			
If it occurs	7	2	8			
When it is an issue	32	82	298			

6. How can the predictions be validated and utilized in a userfriendly manner?

The models are usually validated with the laboratory data used to develop the model. Although user-friendly computer programs have been developed to use the models, the systematic validation of the models based on field operational data is not usually carried out. Because of the complex mechanisms involved and the variability of the experimental data, several models have been developed to predict different aspects of pipeline failure. Because of the dynamic nature of pipeline operations (for example, the fluids transferred through the pipeline change with time), an integrated model that takes into consideration the various operating scenarios of pipelines is essential to predict failures caused by pitting corrosion. To facilitate modelling, as a first approximation, the assumptions made should be validated.

INTEGRATED CORROSION SCIENCE, ELECTROCHEMICAL, AND CORROSION ENGINEERING MODELS

None of the three approaches alone cover all elements of pitting corrosion, but each one of them has a few advantages on certain aspects of pitting corrosion. A comparison of the three model approaches in terms of their ability to characterise pitting corrosion is presented in Table 3.

There is agreement that all failures due to internal corrosion are caused by accumulation of water at critical locations. Further it is important to determine the roles of hydrocarbons (for example, condensates for gas pipelines or hydrocarbons for liquid pipelines), water constituents, and operating parameters (including pressure, temperature, and flow) on pitting corrosion.

Table 3

Comparison of corrosion science, electrochemical science, and corrosion engineering models to predict internal pitting corrosion of oil and gas pipelines.

Question	Corrosion	Electrochemical	Corrosion
	Science	Science	Engineering
If	Yes?	Yes	No
When	Yes?	Yes	No
Where	No	Yes?	Yes?
What	No	Yes	Yes
Which	No	No	Yes
How	No	No	Yes

The next key element is to predict when general corrosion conditions become localized corrosion conditions that result in pipeline failures. Corrosion science models are sufficiently developed to provide this information. Localized corrosion conditions are established when the surface layers are formed.

Once surface layers are formed, the next step is to determine the stability of surface layers. Non-stable surface layers provide conditions for the initiation and propagation of pits. Electrochemical science models are well suited for this purpose. They provide information on electrochemical parameters to predict the probability of initiation and propagation of pits.

In order for the model to be readily used in the field, it is important to predict the occurrence of localized corrosion based on readily available field parameters including steel grade, internal and external pipe diameter, pipe position (horizontal, vertical, or inclined), temperature, pressure, partial pressure of CO₂, partial pressure of H₂S, concentrations of sulfates, bicarbonates and chlorides, and production rates of oil, water, gas and solid.

Thus by suitably integrating the three models, unified pitting corrosion models can be developed to predict the probability of internal pitting corrosion of oil and gas pipelines.

SUMMARY

- Because the laboratory experiments to develop the models are of shorter duration, localized pitting corrosion (the main cause of failure in the field) is not observed and is thus not taken into consideration in corrosion science models. Within the limitations of the models reviewed, the corrosion science models can predict when the surface layers will be formed (and hence conditions for the initiation and propagation of pits can occur), but not where in the pipeline the first failure might occur.
- The electrochemical science models are based on solid scientific principles and carefully carried out laboratory experiments, but because the laboratory experiments carried out to develop the models are not relevant to oil and gas pipeline-operating conditions, these models cannot be readily used. Within the scientific limitations of the models, they can be used to integrate the experimentally determined conditions for surface-layer formation (in the corrosion science models) into other aspects of pitting corrosion. Therefore electrochemical models can predict the probability of pit initiation and propagation, and hence, when the first failure might occur.
- No single operational parameter (such as pipe flow, inclination, pressure, and H₂S partial pressure) can be correlated with pipeline failure. However using the parameters measured in the field in the corrosion science and electrochemical science models, the reliability of predicting the first failure can be improved.
- Based on the comparison of corrosion science, electrochemical science, and corrosion engineering models, it is concluded that no single approach is sufficient to predict internal pitting corrosion of oil and gas pipelines. An integrated, unified model incorporating advantages of all three model approaches could be used to predict internal pitting corrosion more accurately than the current approach of relying on only one model type.

REFERENCES

- M.B. Kermani, L.M. Smith, "CO₂ Corrosion Control in Oil and Gas Production: Design Considerations," European Federation of Corrosion Publications, Number 23, EFC, 1997.
- 2. http://ops.dot.gov/stats2004/.

- 3. Alberta Energy Utilities Board, Canadian report, Statistical Series 57, July 2002.
- 4. Canadian Standards Association (CSA), Standard Z662.2003.
- CAPP Technical Document, "Recommended Practice for Mitigation of Internal Corrosion in Sweet Gas Gathering System", 2002-001, February 2002.
- CAPP Technical Document, "Recommended Practice for Mitigation of Internal Corrosion in Sour Gas Gathering System", 2003-0023, January 2003.
- S. Papavinasam, R.W. Revie, and A. Doiron, "Predicting Internal Pitting Corrosion of Oil and Gas Pipelines: Review of Corrosion Science Models," NACE CORROSION 2005, Paper #5643, Houston, Texas, 2005.
- 8. S. Papavinasam, R.W. Revie, and A. Doiron, "Predicting Internal Pitting Corrosion of Oil and Gas Pipelines: Review of Electrochemical Models," NACE CORROSION 2005, Paper #5645, Houston, Texas, 2005.
- S. Papavinasam, W. Friesen, R.W. Revie, and A. Doiron, "Predicting Internal Pitting Corrosion of Oil and Gas Pipelines: Review of Corrosion Engineering Approach," NACE CORROSION 2005, Paper #5646, Houston, Texas, 2005.
- C. de Waard, D.E. Milliams, "Carbonic Acid Corrosion of Steel," Corrosion, NACE, Vol 31, No. 5, 177-181, May 1975.
- 11. C. de Waard, U. Lotz, "Prediction of CO2 Corrosion of Carbon Steel," NACE CORROSION 93, Paper #69, Houston, Texas, 1993.
- C. de Waard, U. Lotz, and A. Dugstad, "Influence of Liquid Flow Velocity on CO₂ Corrosion: A Semi-Empirical Model," NACE CORROSION 95, Paper #128, Houston, Texas, 1995.
- 13. S. Srinivasan, R.D. Kane, "Prediction of Corrosivity of CO₂/H₂S Production Environments," NACE CORROSION 96, Paper #11, Houston, Texas, 1996.
- M.R. Bonis, J.L. Crolet, "Basics of the Prediction of the Risks of CO₂ Corrosion in Oil and Gas Wells," NACE CORROSION 89, Paper #466, Houston, Texas, 1989.
- 15. J.-L. Crolet, N. Thevenot, and A. Dugstad, "Role of Free Acetic Acid on the CO₂ Corrosion of Steels," NACE CORROSION 99, Paper #24, Houston, Texas, 1999.
- S. Nesic, J. Postlethwaite, and S. Olsen, "An Electrochemical Model for Prediction of Corrosion in Mild Steel in Aqueous Carbon

- Dioxide Solutions," Corrosion Vol. 52, No. 4, 280, 1996.
- S. Nesic, J. Postlethwaite, and S. Olsen, "An Electrochemical Model for Prediction of CO₂ Corrosion," NACE CORROSION 95, Paper #131, Houston, Texas, 1995.
- S. Nesic, M. Nordsveen, R. Nyborg, and A. Stangeland, "A Mechanistic Model for CO₂ Corrosion with Protective Iron Carbonate Films," Corrosion 2001, Paper #01040.
- B. Mishra, S. Al-Hassan, D.L. Olson, and M.M. Salama, "Development of a Predictive Model for Activation-Controlled Corrosion of Steel in Solutions Containing Carbon Dioxide," Corrosion, Vol 53, No. 11, 852-859, Nov. 1997.
- A. Anderko, R. D. Young, "Simulation of CO2/H2S Corrosion using Thermodynamic and Electrochemical Models," NACE CORROSION 99, Paper #31, Houston, Texas.
- A. Anderko, "Simulation of FeCO3/FeS Scale Formation Using Thermodynamic and Electrochemical Models," NACE CORROSION 2000, Paper #00102, Houston, Texas.
- 22. A. Anderko, P. McKenzie, and R.D. Young, "Computation of Rates of General Corrosion Using Electrochemical and Thermodynamic Models," Corrosion, Vol 57, No. 3, 202-213, March 2001.
- 23. J.E. Oddo, M.B. Thompsons, "The Prediction of Scale and CO2 Corrosion in Oil Field Systems," NACE CORROSION 99, Paper #41, Houston, Texas, 1999.
- E. Dayalan, F.D. de Moraes, J.R. Shadley, S.A. Shirazi, and E.F. Rybicki, "CO2 Corrosion Prediction in Pipe Flow under FeCO3 Scale-Forming Conditions," NACE CORROSION 98, Paper #51, Houston, Texas, 1998.
- 25. B.F.M. Pots, "Mechanistic Models for the Prediction of CO2 Corrosion Rates under Multiphase Flow Conditions," NACE CORROSION 95, Paper #137, Houston, Texas, 1995.
- M.B. Kermani, L.M. Smith, "CO2 Corrosion Control in Oil and Gas Production, Design Considerations," European Federation of Corrosion Publications, Number 23, Chapter 6, 18-23, 1997.
- C.D. Adams, J.D. Garber, and R.K. Sing, "Computer Modelling to Predict Corrosion Rates in Gas Condensate Wells Containing CO2," NACE CORROSION 96, Paper #31, Houston, Texas, 1996.
- 28. R. Nyberg, P. Andersson, and M. Nordsveen, "Implementation of CO2 Corrosion Models in a Three-Phase Fluid Flow Model," NACE CORROSION 2000, Paper #48, Houston, Texas, 2000.

- 29. A.M.K. Halvorsen, T. Sontvedt, "CO2 Corrosion Model for Carbon Steel Including a Wall Shear Stress Model for Multiphase Flow and Limits for Production Rate to Avoid Mesa Attack," NACE International, CORROSION 99, Paper #42, Houston, Texas, 1999.
- "CO₂ Corrosion Rate Calculation Model," NORSOK Standard # M-506, Norwegian Technology Standards Institution, http://www.nts.no/norsok, Oslo, 1998.
- 31. N.F. Mott, Trans. Faraday Soc., 43 (1947), p. 429; J. Chim. Phys.44, 172, 1947.
- 32. G.L. Griffin, Journal of the Electrochemical Society, 131, p. 18, 1984.
- 33. M. Fleischmann and H.R. Thirsk, Journal of the Electrochemical Society, 110, p. 688, 1963.
- 34. N. Sato and M. Cohen, Journal of the Electrochemical Society, 111, p. 512, 1964.
- 35. C. Sarasola, T. Fernandez, and Y. Jimenez, Electrochimica Acta, 33, p. 1295, 1988.
- 36. D. Devilliers, F. Lantelme and M. Chemla, Electrochimica Acta, 31, p. 1235, 1986.
- 37. C.Y. Chao, L.F. Lin, and D.D. Macdonald, Journal of the Electrochemical Society, 128, p. 1187 and 1194, 1981.
- 38. J.R. Ambrose, "Treatise on Materials Science and Technology," Vol. 23, p. 175, 1981.
- 39. S.M. Sharland, "A Review of the Theoretical Modelling of Crevice and Pitting Corrosion", Corrosion Science, 27(3), p. 289-323, 1987.
- 40. T. Okada, Journal of the Electrochemical Society, 132, p. 537, 1985.
- 41. T. Shibata, Corrosion Science, 33, p. 1633, 1992.
- 42. T.M. Sharland, C.M. Bishop, P.H. Ballkwill, and J. Stewart, "Advances in Localized Corrosion: Proceedings of the Second International Conference on Localized Corrosion," p. 109, 1987.
- 43. B. Baroux, Corrosion Science, 28, p. 969, 1988
- 44. R.C. Salvarezza, N.D. Cristofaro, C. Pallotta, and A.J. Arvia, Electrochimica Acta, 32, p. 1049, 1987.
- 45. K. Hebert, R. Alkire, Journal of the Electrochemical Society, 130, p. 1007, 1983.
- 46. D.E. Williams, C. Westcott, and M. Fleischmann, Journal of the Electrochemical Society, 132, p. 1796 and 1804, 1985.
- 47. U. Bertocci, "Advances in Localized Corrosion," Proceedings of the Second International Conference on Localized Corrosion, p.127,

1987.

- 48. .W. Oldfield, W.H. Sutton, British Corrosion Journal, 13, p. 13, 1978.
- 49. Y. Xu, M. Wang, and H.W. Pickering, Journal of the Electrochemical Society, 140, p. 3448, 1993.
- 50. Y. Xu, H.W. Pickering, Journal of the Electrochemical Society, 140, p. 658, 1993.
- 51. R.S. Lillard, J.R. Scully, Journal of the Electrochemical Society, 141, p. 3006, 1994.
- 52. J.A. Bardwell, J.W. Fraser, B. MacDougall, and M.J. Graham, "Influence of the Anodic Oxide Film on Pitting of Iron," Journal of the Electrochemical Society 139, p. 366, 1992.
- 53. J.L. Dawson, M.G.S. Ferreira, "Electrochemical Studies of the Pitting of Austenitic Stainless Steel," Corrosion Science 26, p. 1009, 1986.
- K. Hebert, R. Alkire, "Dissolved Metal Species Mechanism for Initiation of Crevice Corrosion of Aluminum: II. Mathematical Model," The Journal of the Electrochemical Society, 130, p. 1007, 1983.
- 55. E. McCafferty, "A Competitive Adsorption Model for the Inhibition of Crevice Corrosion and Pitting," Journal of the Electrochemical Society, 137, p. 3731, 1990.
- D.D. MacDonald, M.U. MacDonald, "Theory of Steady-State Passive Films," Journal of the Electrochemical Society, 137, p. 2395, 1990.
- 57. D.D. MacDonald, M.U. MacDonald, "Distribution Functions for the Breakdown of Passive Films," Electrochimica Acta, 31, p. 1079, 1986.
- 58. T. Nagatani, Journal of the Physical Society of Japan, 60, p. 3997, 1991.
- 59. G.R. Matamala, Corrosion, 43, p. 97, 1987.
- 60. W.H. Smyrl, J. Newman, Journal of the Electrochemical Society, 121, p. 1000, 1974.
- 61. J.C. Fan, J. Richardson, Corrosion Conference/94, Paper 315.
- 62. E.E. Molo, B. Mellein, E.M.R.D. Schiapparelli, J.L. Vicente, R.C. Salvarezza, and A.J. Arvia, Journal of the Electrochemical Society, 137, p. 1384, 1990.
- 63. J.W. Tester, H.S. Issac, Journal of the Electrochemical Society, 122, p. 1438, 1975.

- 64. T.R. Beck, R.C. Alkire, "Occurrence of Salt Films during Initiation and Growth of Corrosion Pits," Journal of the Electrochemical Society, 126, p. 1662, 1979.
- 65. B.G. Ateya, H.W. Pickering, Journal of the Electrochemical Society, 122, p. 1018, 1975.
- 66. A. Ben Rais, J.C. Sohm, Corrosion Science, 25, p. 1047, 1985.
- 67. P. Doig, P.E.J. Flewit, Proc. R. Soc., A357, p. 439, 1977.
- 68. P. Doig, P.E.J. Flewit, Metall. Trans., 9A, p. 357, 1978.
- 69. B.H. Melville, Brit. Corr. J, 14, p. 15, 1979.
- 70. J.M. Galvele, Journal of the Electrochemical Society, 123, p. 464, 1976.
- 71. J.M. Galvele, Corrosion Science, 21, p. 551, 1981.
- 72. S.M. Gravano, J.R. Galvele, Corrosion Science, 24, p. 517, 1984.
- 73. R. Alkire, D. Ernsberger, and D. Damon, Journal of the Electrochemical Society, 123, p. 458, 1976.
- 74. ASTM G170, "Standard Guide for Evaluating and Qualifying Oilfield and Refinery Corrosion Inhibitors in the Laboratory," 100 Barr Harbor Drive, West Conshohocken PA, USA, 19428, 2001.
- 75. J.Y. Sun, and W.P. Jepson, "Slug Flow Characteristics and their Effect on Corrosion in Horizontal Oil and Gas Pipelines," SPE 24787, 67th Annual Technical Conference Society of Petrol Engineering, Washington, 1992.
- J.M. Mandhane, G.A. Gregory, and K. Aziz, "A Flow Pattern Map for Gas-liquid Flow in Horizontal Pipes," Int. J. Multiphase Flow 1, 537, 1974.
- 77. G. Hetsroni, "Handbook of Multiphase Systems," Hemisphere Publications, Washington, 237, 1982.
- 78. A. Miller, "Pipeline Corrosion and Corrosion Control in Sour Devonian Multiphase Production," NACE Northern Area Eastern Conference and Exhibition, Paper No. 2A.2, Ottawa, Ontario, Canada, Oct. 24-27, 1999.
- 79. Failure Data of Oil Production Pipelines, CANMET Division Report, WRC, 96-27 (CF) 1995.
- 80. R. Jasinski, "Corrosion of N80-Type Steel by CO₂ /Water Mixtures", Corrosion, NACE, Vol 43, No. 4, 214-218, April 1987.
- S. Tebbal, N. Hackerman, "Effect of the Liquid Film Thickness on the CO2 Corrosion of Steel", Corrosion, Vol 45, No. 7, 558-562, July 1989.

- A. Ikeda, M. Ueda, and S. Mukai, "CO₂ Behavior of Carbon and Cr Steels", Advances in CO₂ Corrosion, Vol 1, Corrosion 83, 39-51, 1983.
- K. Masamura, S. Hashizume, K. Nunomura, J. Sakai, and I. Matsushima, "Corrosion of Carbon and Alloy Steels in Aqueous CO2 Environments", Advances in CO₂ Corrosion, Vol. 1, Corrosion 83, 143-150, 1983.
- 84. E. B. Backensto, R. E. Drew, and C. C. Stapleford, "High Temperature Hydrogen Sulfide Corrosion", Corrosion, Vol 12, No. 1, 22-31, 1956.
- 85. G. Schmitt, "Fundamental Aspects of CO2 Corrosion", Advances in CO2 Corrosion, Vol 1, Corrosion 83, 10-19, 1983.
- 86. S.T. Adamy, F.R. Cala, "Inhibition of Pitting in Ferrous Materials by Carbonate as a Function of Temperature and Alkalinity", Corrosion, Vol 55, No. 9, 825-839, September 1999.
- 87. J.R. Bryant, G.B. Chitwood, "Corrosion Behaviour of 1 to 22% Chromium Steels and Monel K-500 in CO₂ Brine Environments", Advances in CO₂ Corrosion, Vol 1, Corrosion 83, 163-171, 1983.
- 88. A. Hafeez, E.T. Wanderer, "Aluminum Alloys for Use in CO₂ Enhanced Oil Recovery (EOR) Systems", Advances in CO₂ Corrosion, Vol 2, Corrosion 84/85, 113-132, 1985.
- 89. D.V. Satyanarayana Gupta, "Effect of pH and Sulphide Ion Concentration in Aqueous Neutral and Alkaline Solution at Room Temperature", Corrosion, Vol 37, No. 11, 611-616, 1981.
- H.S. Gadiyar, N.S.D. Elayathu, "Corrosion and Magnetite Growth on Carbon Steels in Water at 310 C- Effect of Dissolved Oxygen, pH, and EDTA Addition", Corrosion, Vol 36, No. 6, 306-312, 1980.
- 91. R.H. Hausler, "The Mechanism of CO₂ Corrosion of Steel in Hot, Deep Gas Wells", Advances in CO₂ Corrosion, Vol 1, Corrosion 83, 72-86, 1983.
- 92. M. Onoyama, K. Shitani, N. Hayashi, M. Murata, "Resistance of Some High Alloys to CO₂-H₂S Corrosion at Elevated Temperatures", Advances in CO₂ Corrosion, Vol 2, Corrosion 84/85, 72-79, 1985.
- 93. A. Ikeda, S. Mukai, and M. Ueda, "Corrosion Behavior of 9 to 25% Cr Steels in Wet CO₂ Environments", Advances in CO₂ Corrosion, Vol 2, Corrosion 84/85, 47-54, 1985.
- 94. A. Dugstad, "Mechanism of Protective Film Formation During CO2 Corrosion of Carbon Steel", Corrosion 98, Paper #31, 1998.

- B. Lefebvre, G. Guntz, J.J. Prouheze, J.J. Renault, and P. Bounie, "Behaviour of Carbon Steel and Chromium Steels in CO2 Environments", Advances in CO2 Corrosion, Vol 2, Corrosion 84/85, 55-71, 1985.
- 96. C. Manfredi, T.A. Mozhi, and B.E. Wilde, "Corrosion of Carbon Steel in Saturated Brine at 150 C The Effect of pH", Corrosion, Vol 45, No. 3, 172-177, 1989.
- 97. W. McLeod, R.R. Rogers, "Sulfurous Acid Corrosion of Low Carbon Steel at Ordinary Temperatures I. Its Nature", Corrosion, Vol 22, 143-146, 1966.
- 98. K. Masamura, S. Hashizume, J. Sakai, T. Ono, and I. Matsushima, "Pitting Corrosion Resistance of High-Alloy OCTG in CO₂ Environment as Affected by Chlorides and Sulfides", Advances in CO₂ Corrosion, Vol 2, Corrosion 84/85, 80-95, 1985.
- B.D. Craig, "The Nature of Iron Sulfides Formed on Steel in an H₂S-O₂ Environment", Corrosion, Vol 35, No. 3, 136-138, 1979.
- 100. J.N. Al-Hajji, M.R. Reda, "Corrosion Behavior of Low-Residual Carbon Steels in a Sour Environment", Corrosion, Vol 49, No. 5, 363-371, 1993.
- 101. C.D. Waard, U. Lotz, "Prediction of CO2 Corrosion of Carbon Steel", Corrosion 93, Paper #69, 1993.
- 102. E. Heitz, "Chemo-Mechanical Effects of Flow on Corrosion", Corrosion, Vol 47, No. 2, 135-145, 1991.
- G. Schmitt, B. Rothmann, "Corrosion of Unalloyed and Lowalloyed Steels in Carbonic Acid Solutions", Werkstoffe und Korrosion, Vol. 29, 237, 1978.
- 104. J.A. Dougherty, "Corrosion Inhibition of Wet, Sour Gas Lines Carrying Elemental Sulfur", Corrosion 92, Paper #2, 1992.
- 105. J.W. Slusser, S.W. Dean, and W.R. Watkins, "CO Inhibition of Wet CO2 Corrosion of Carbon Steel", Materials Performance, 40-45, January 1997.
- 106. P. Chatterjee, D.D.N. Singh, "Inhibitive Effect of Octyl Amines in Hydrogen Sulphide Solution", J. Electrochem. Soc., India, 1989.
- 107. S.W. Dean, "Velocity Accelerated Corrosion Testing and Predictions", Materials Performance, 61-67, September 1990.
- 108. R. Nyborg, A. Dugstad, "MESA Corrosion Attack in Carbon Steel and 0.5% Chromium Steel", Corrosion 98, Paper #29, 1998.
- 109. K. Satoh, K. Yamamoto, and N. Kagawa, "Prevention of CO2

- Corrosion in Gas Gathering Systems", Advances in CO₂ Corrosion, Vol 1, Corrosion 83, 151-156, 1983.
- 110. A. Ikeda, M. Ueda, and S. Mukai, "Influence of Environmental Factors on Corrosion in CO₂ Source Well", Advances in CO₂ Corrosion, Vol 2, Corrosion 84/85, 1-22, 1985.
- 111. K. Videm, A. Dugstad, "Corrosion of Carbon Steel in an Aqueous Carbon Dioxide Environment Part 2: Film Formation", Material Performance, 46-50, April 1989.
- 112. G. Schmitt, W. Bruckhoff, "Inhibition of Low and High Alloy Steels in the System Brine/Elemental Sulfur/H₂S", NACE, Corrosion 89, Paper #620, 1989.
- 113. E.C. Greco, W.B. Wright, "Corrosion of Iron in an H₂S-CO₂-H₂O System", Corrosion, Vol 18, 119-124, 1962.
- R.L. Tapping, P.A. Lavoie, and R.D. Davidson, "Effect of Neutralization on Protectiveness of Sulfide Film on Carbon Steel", Materials Performance (9), 43-47, 1983.
- A.L. Cummings, F.C. Veatch, A.E. Keller, "Corrosion and Corrosion Control Methods in Amine Systems Containing Hydrogen Sulfide", Materials Performance, 42-47, January 1998.
- 116. R.A. Pisigan, Jr., J.E. Singley, "Evaluation of Water Corrosivity Using the Langlier Index and Relative Corrosion Rate Models", Material Performance-NACE, 26-36, 1985.
- D.L. Johnson, H. Omura, "Characterization of Carbon Steel Corrosion in Dilute Ammonium Nitrate Solutions and Irrigation Ground Waters", Corrosion, Vol 37, No. 4, 209-213, 1981.
- 118. K. Videm, J. Kvarekvaal, T. Perez, and G. Fitzsimons, "Surface Effects on the Electrochemistry of Iron and Carbon Steel Electrodes in Aqueous CO₂ Solutions", Corrosion 96, Paper #1, 1996.
- 119. A. Dugstad, "The Importance of FeCO₃ Supersaturation on the CO₂ Corrosion of Carbon Steels", Corrosion 92, Paper #14, 1992.
- 120. A. Dugstad, H. Hemmer, and M. Seiersten, "Effect of Steel Microstructure on Corrosion Rate and Protective Iron Carbonate Film Formation", Corrosion, Vol 57, No. 4, 369-378, April 2001.
- 121. J.L. Crolet, M.R. Bonis, "The Very Nature of the CO₂ Corrosion of Steels in the Oil and Gas Wells and the Corresponding Mechanisms", Oil/Gas European Magazine, Vol 10, No. 2, 68-76, 1984.
- 122. T. Hara, H. Asahi, Y. Suehiro, and H. Kaneta, "Effect of Flow

- Velocity on Carbon Dioxide Corrosion Behavior in Oil and Gas Environments", Corrosion, Vol 56, No. 8, 860-866, August 2000.
- 123. R.H. Hausler, D.W. Stegmann, C.I. Cruz, and D. Tjandroso, "Laboratory Studies on Flow Induced Localized Corrosion in CO₂/H₂S Environments, II. Parametric Study on the Effects of H₂S, Condensate, Metallurgy, and Flowrate", Corrosion 90, Paper #6, 1990.
- 124. G. Schmitt, D. Steinmetz, and W. Bruckhoff, "Unexpected Alloying Influences in Connection with the Corrodibility of Sour Gas Delivery Pipes", Workstoffe und Korrosion 36, 309-315, 1985.
- 125. M.W. Joosten, T. Johnsen, A. Dugstad, T. Walmann, T. Jossang, P. Meakin, and J. Feder, "In-Situ Observation of Localized CO2 Corrosion", Corrosion 94, Paper #3, 1994.
- 126. M. Matsui, A. Kuhara, A. Yoshitake, and T. Ishii, "The Development of High Strength 12% Cr Centrifugally Cast Pipe for Gas Gathering Piping Systems", Advances in CO₂ Corrosion, Vol 1, Corrosion 83, 130-142, 1983.
- 127. C.D. Waard, D.E. Milliams, "Carbonic Acid Corrosion of Steel", Corrosion, Vol 31, No. 5, 177-181, 1975.
- 128. G. Schmitt, C. Bosch, U. Pankoke, W. Bruckhoff, and G. Siegmund, "Evalution of Critical Flow Intensities for FILC in Sour Gas Production", Corrosion 98, Paper #46, 1998.
- 129. J.W. Graydon, D.W. Kirk, "Corrosion of Carbon Steel in Aqueous Lithium Hydroxide", Corrosion, Vol 46, No. 12, 1002-1006, 1990.
- 130. V. Subramanian, W.J. Van Ooij, "Effect of the Amine Functional Group on Corrosion Rate of Iron Coated with Films of Organofunctional Silanes", Corrosion, Vol 54, No. 3, 204-215, 1998.
- 131. J.M. Ahao, Y. Zuo, "Pitting Corrosion of Steel Pipeline in Oil-Water-Gas Multiphase Flow System", British Corrosion Journal 2000, Vol 35, No. 1 73-74, 2000.
- 132. M. Ueda, A. Ikeda, "Effect of Microstructure and Cr Content in Steel on CO2 Corrosion", Corrosion 96, Paper #13, 1996.
- 133. H.U. Schutt, P.R. Rhodes, "Corrosion in an Aqueous Hydrogen Sulfide, Ammonia, and Oxygen System", Corrosion, Vol 52, No. 12, 947-952, 1996.
- 134. H. Takabe, M. Ueda, "The Formation Behavior of Corrosion Protective Films of Low Cr Bearing Steels in CO₂ Environments", Corrosion 2001, Paper #01066, 2001.

- U. Lotz, T. Sydberger, "CO₂ Corrosion of Carbon Steel and 13Cr Steel in Particle-laden Fluid", Corrosion, Vol 44, No. 11, 800-809, November 1988.
- S. Nesic, L. Lunde, "Carbon Dioxide Corrosion of Carbon Steel in Two-phase Flow", Corrosion, Vol 50, No. 9, 717-727, September 1994.
- 137. S. Nesic, M. Nordsveen, R. Nyborg, and A. Stangeland, "A Mechanistic Model for CO₂ Corrosion with Protective Iron Carbonate Films", Corrosion 2001, Paper #01040, 2001.
- 138. A. Hedayat, J. Postlehwaite, and S. Yannacopoulos, "Conjoint Action of CO₂ Corrosion and Reciprocating Sliding Wear on Plain Carbon Steel Part II – Electrochemical Studies", Corrosion, Vol 48, No. 12, 1027-1031, 1992.
- 139. K. Videm, J. Kvarekval, "Corrosion of Carbon Steel in Carbon Dioxide-Saturated Solutions Containing Small Amounts of Hydrogen Sulfide", Corrosion, Vol 51, No. 4, 260-269, April 1995.
- 140. D.C. Bond, G.A. Marsh, "Corrosion of Wet Steel by Hydrogen Sulfide-Air Mixtures", Corrosion, Vol 6, No. 1, 22-28, 1950.
- 141. B.D. Craig, "The Occurrence of Cementite as a Corrosion Product at Low Temperatures [50°C (120°F)] in a Gas Environment", Materials Performance, 34-37, February 1977.
- 142. P. Mayer, A.V. Manolescu, and M. Rasile, "Corrosion of Medium Carbon Steel in Aqueous Solution Containing Fluoride Ions at 300 C", Corrosion, Vol 40, No. 4, 186-189, 1984.
- 143. K.J. Kennelley, S.N. Smith, and T.A. Ramanarayanan, "Effect of Elemental Sulfur on the Performance of Nitrogen-Based Oilfield Corrosion Inhibitors", Materials Performance, 48-52, February 1990.
- 144. F.D. De Moraes, "Characterization of CO₂ Corrosion Product Scales Related to Environmental Condition", Corrosion 2000, Paper #00030, 2000.
- 145. E. Gulbrandsen, R. Nyborg, T.Loland, and K. Nisancioglu, "Effect of Steel Microstructure and Composition on Inhibition of CO₂ Corrosion", Corrosion 2000, Paper #00023, 2000.
- J. Crolet, N. Thevenot, and A. Dugstad, "Role of Free Acetic Acid on the CO2 Corrosion of Steels", Corrosion 99, Paper #24, 1999.
- 147. B. Hedges, L. Mcveigh, "The Role of Acetate in CO₂ Corrosion: The Double Whammy", Corrosion 99, Paper #21, 1999.

- R.L. Martin, R.R. Annand, "Accelerated Corrosion of Steel by Suspended Iron Sulfides in Brine", Corrosion, Vol 36, No. 5, 297-301, 1980.
- 149. W.P. Jepson, "The Effect of Flow Characteristics on Sweet Corrosion in High-Pressure, Three-Phase, Oil/Water/Gas Horizontal Pipelines", Prevention of Pipeline Corrosion Conference, 1994.
- 150. G. Schmitt, W. Bruckhoff, "Inhibition of Low and High Alloy Steels in the System Brine/Elemental Sulfur/H₂S", NACE, Corrosion 89, Paper #620, 1989.
- 151. J.L. Crolet, S. Olsen, and W. Wilhelmsen, "Influence of a Layer of Undissolved Cementite on the Rate of the CO₂ Corrosion of Carbon Steel", Corrosion 94, Paper #4, 1994.
- 152. J.K. Heuer, J.F. Stubbins, "Microstructure Analysis of Coupons Exposed to Carbon Dioxide Corrosion in Multiphase Flow", Corrosion, Vol 54, No. 7, 566-575, July 1998.
- 153. C.A. Palacios, J.R. Shadley, "CO₂ Corrosion of N-80 Steel at 71°C in a Two-phase Flow System", Corrosion, Vol 49, No. 8, 686-693, August 1993.
- 154. S. Srinivasan, R.D. Kane, "Prediction of Corrosivity of CO₂/H₂S Production Environments", Corrosion 96, Paper #11, 1996.
- 155. T.A. Ramanarayanan, S.N. Smith, "Corrosion of Iron in Gaseous Environments and in Gas-Saturated Aqueous Environments", Corrosion, Vol 46, No. 1, 66-74, 1990.
- 156. C.D. Waard, U. Lotz, and A. Dugstad, "Influence of Liquid Flow Velocity on CO₂ Corrosion: A Semi-Empirical Model", Corrosion 95, Paper #128, 1995.
- 157. K. Videm, A. Dugstad, "Corrosion of Carbon Steel in an Aqueous Carbon Dioxide Environment Part 1: Solution Effects", Material Performance, 63-67, April 1989.
- 158. A.K. Dunlop, H.L. Hassell, and P.R. Rhodes, "Fundamentals Considerations in Sweet Gas Well Corrosion, Advances in CO₂ Corrosion", Corrosion 83, 52-63, 1983.
- 159. K. Mabuchi, Y. Horii, H. Takahashi, and M. Nagayama, "Effect of Temperature and Dissolved Oxygen on the Corrosion Behavior of Carbon Steel in High-Temperature Water", Corrosion, Vol 47, No. 7, 500-508, 1991.
- J. Jelinek, P. Neufeld, "Kinetics of Hydrogen Formation from Mild Steel in Water under Anaerobic Conditions", Corrosion, Vol 38, No.

2, 98-104, 1982.

161. NACE Report 3T199: "Techniques for Monitoring Corrosion Related Parameters in Field Applications", 1999.